

Design Team Number: 04

Design Team Title: Sensor Scavenging

FINAL DESIGN REPORT

Team Members: Josh Mahaffey

Ben McDonald

Jeff Petermann

Jacob Pozderac

Faculty Advisor: Dr. Giakos

Date Submitted: 4/27/2009

Table of Contents

Abstract	1
1.0) Introduction	2
1.1) Statement of Needs	2
2.2) Problem Definition	2
2.3) Goal	2
2.4) Constraints	2
2.0) Design Specifications	3
2.1) Base Station	3
2.2) Data Node	4
2.3) Sensing Node	5
3.0) Accepted Technical Design	6
3.1) Solar Panel Array and Tracking Control	7
3.2) Flyback Power Supply and Battery Bank	14
3.3) Base Station Communication and Interface Software ..	22
3.4) Sensor Node	26
4.0) Service/Maintenance Instructions & Operations Manual	38
4.1) Operations Manual	40
5.0) Testing Procedure	41
5.1) Base Station Testing Procedure	41
5.2) Sensor Node Testing Procedure	42
5.3) Software Testing Procedure	44
5.0) Financial Budget	44
5.1) Labor Costs	44
5.2) Material Costs	45
6.0) Project Schedule	48
A) Matlab Scripts and Plots for Power Supply and Panels	a
B) Mechanical Considerations	e

List of Figures

1)	Detailed Block Diagram of System	6
2)	General Problem of Incident Power (Stationary Panel)	7
3)	Transformed Problem of Incident Power	8
4)	Incident Power Density and Energy Comparisons	8
5)	Solar Panel Array Control Circuit	9
6)	Solar Panel Array and Hardware Implementation	9
7)	Solar Panel/Stepper Motor Wiring and Communication Diagram	10
8)	Solar Panel Control Software Flow Diagram	12
9)	Pseudo-code for Solar Panel Control Software	13
10)	Block Diagram of Base Station Power Unit	15
11)	Solar Panel Model	17
12)	Converter Input Impedance as a Function of T_s and Duty Cycle	18
13)	Converter Performance with Analysis of MPP Contribution	19
14)	Average Current Measurement Using Sense Resistor	20
15)	Power Converter Schematic	21
16)	PCB Layout of the Base Station Power Supply	21
17)	Implementation Picture of Flyback Power Supply	22
18)	Software Block Diagram	22
19)	MAC Protocol Implemented in Each Transmission	24
20)	Base Station Communication Flow Diagram	25
21)	Base Station Communication Pseudo-code	26
22)	Process Message Pseudo-code	27
23)	Overall Sensing Circuit Block Diagram	27
24)	Overall Circuit Schematic of Sensor Node	30
25)	PCB Layout of the Sensor Node Board	31
26)	Picture of the Hardware at the Sensor Node	31
27)	Software Flow Diagram for the Sensor Nodes	34
28)	Pseudo-code for Sensor Node Software	35
29)	SPI and I/O Output of CC2430 and SCP 1000 Sensor	36
30)	Current Consumption Profile of the Sensor Node	37
31)	Battery Life Profile for Various Cycle Times	37
32)	Assembly Diagrams and Photographs	38
33)	Power Supply Mount and Enclosure	39
34)	Block Diagram Showing Wired Connections	40
35)	Alternative Sensing Node Charging Circuit	43
36)	Testing Procedure Flow to Verify Sensor Node Operation	40
37)	Sensor Node Peripheral and GPIO Reading	45
38)	Project Design Schedule	47
39)	Project Implementation and Prototype Schedule	50

List of Tables

1)	Solar Panel Array and Control Module	10
2)	Distribution of Amp-Hour Usage at Base Node	19
3)	Costed Bill of Materials of Power Supply	21
4)	Sensing Node Module	27
5)	Sensor Node Hardware Parts List	29
6)	Labor Cost	41
7)	Parts and Materials Cost	42

Abstract

Wireless sensing networks are becoming increasingly common throughout industry, medicine, and consumer electronics. They advantageously allow users to monitor a multitude of information from a single location, typically referred to as the interrogating unit. Individual sensing nodes transmit relevant data back to the interrogator for analysis. The advantage of this hierarchy is that large numbers of sensors can be added to the system with little adjustment.

For industrial applications, the size and nature of the sensing nodes is flexible in terms of power sources and placement. However, other applications, such as space exploration, require placement of sensors in locations that are inaccessible by wiring or power sources. In such a system the sensing nodes are ideally passive or rely solely on received RF energy to perform all operations. A further improvement to traditional sensing networks that would allow for applications in space would be to utilize a standardized communication protocol. This would allow for further expansion of the sensing network. The challenge of incorporating a standard communications protocol in the ideal sensor is that it requires increased transmission times, and hence greater power usage.

The goal of this project is to develop a sensing network that uses a standard communications protocol with sensing nodes that are not constrained by direct wiring or independent power sources. The method will be demonstrated with temperature and pressure sensors; however any desired parameters could be incorporated. The total system will consist of a base station for setting adjustment and monitoring, an intermediate data node used for the short distance transmission of RF energy, and sensing nodes that will monitor the environmental conditions on and surrounding the astronauts.

1.0) Introduction

The significance of a particular advancement in technology is not often fully recognized until it is merged with other technologies to create new possibilities. One such case has been the development of sensing networks. The combination of three areas of research has produced a new paradigm of possibilities.

First, many wireless communication protocols have adapted an “ad-hoc” hierarchy. In an ad-hoc network, individual devices, or nodes, work cooperatively to pass data through the network. This decreases the burden on the nodes in terms of power and transmission requirements. Secondly, the advent of many low power and even passive sensors has made the acquisition of environmental data easier. These sensors are less constrained in terms of where they may be placed given their minimal power requirements. Third, successful deployment of miniaturized nodes in industrial applications, such as RFID, has provided an example of the value that can be added to a process and resulting economic viability. This project combines these three principles in the specific application of space exploration.

1.1) Statement of Need:

This project is being underwritten by NASA to specifically explore the possibility of combining a low power or passive sensing network with existing (mature) wireless protocols. The advantage of this is to expand the range over which a network can exist to a potentially unlimited number of sensing nodes and the added robustness of a actively supported communications standard. Lastly, it also standardizes the requirements necessary for deployment.

1.2) Problem Definition:

With the addition of a robust wireless protocol brings the challenge of increased power requirements. Sensing nodes need to be deployed in an ad-hoc fashion which is dynamic. For the purposes of this prototype however, a specific function will be examined. The sensing node locations will be assumed to be on equipment, gear (i.e. space suit), or astronauts themselves. Astronauts may however not be necessarily located within close proximity to other astronauts or sensing nodes.

1.3) Goal:

The goal of this project is to incorporate a low power or passive-natured sensor network utilizing the Zigbee protocol.

1.4) Constraints:

The prototype will have the capability to monitor sensors within a 75m range initially. Sensors will be free from external wiring and small enough in nature to mount anywhere within a space suit. Two specific parameters will be used for trial; however the focus will be on the network implementation and could be expanded to suite a wide variety of collected data.

2.0) Design Specifications

To achieve the goals and overcome the constraints outlined in Section 1.0, the following network hierarchy has been conceived:

The sensing network consists of the basic units as shown in Figure [1]:

2.1) Base Station

Drawing its energy from the environment, the station will consist of a display unit and a controller unit allowing the user to view vital information, program update rates, and perform long distance communication. This will provide NASA long range visibility of the network. The base station will be required to communicate with the sensing network itself at a distance of 75m.

2.1.1) Mechanical Design:

- Stepper Motor:
 - 1) Can rotate 6.3 lb panel in 1.8 degree increments
 - 2) Allow full 360 degree rotation.
- Weight: Under 45 lbs so it can be “wheeled” from one location to another.
- Overall Dimensions: 16” x 36”

2.1.2) Power System:

- Solar Panel (SP) Power: 20W
- SP Voltage Range: 6 – 20V
- Battery Life: Completely sustained if panels receive 4 hours of equivalent full irradiation per day.
- Buck/Boost Regulator: Can charge batteries to a nominal voltage of 14.2V from given SP voltage range.

2.1.3) Material Design:

- Outer Enclosure: Will be metallic or some other material that provides RF shielding of the antennas from the internal circuitry.

2.1.4) Control Design:

- Stepper Motor: Motor output must be able to communicate position accurate to within 1.8 degrees.
- Buck/Boost Regulator: Feedback of output voltage and calculations based on A/D measurements from the solar panel will provide data to calculate proper duty cycle for maximum power point tracking and voltage regulation.

2.1.5) Electrical Design:

- User Interface: “One-button” operation of LCD that displays sensor network information.
- Inter System Comm.: Utilize SPI communications to support multiple processors.

2.1.6) Radiation Design:

- Transmit Distance: 75 meters

2.1.7) Economic/Ergonomic:

- Wheeled Enclosure: To effectively move 45 lbs easily the structure shall be wheeled.
- Transportability: External features such as antennas and the solar panel shall be attachable/detachable to allow for easier transportation.

2.2) Data Node **

Due to the small size of the sensing nodes, they will not have sufficient resources to transmit 75m with the added constraint of using the Zigbee protocol reliably. The Data Node will handle processing of the passive nodes and have sufficient power to transmit back to the base. Although in the proposed scenario it may not be feasible to always have the base station in close proximity to the sensing nodes, it is reasonable to assume that there may be some provision for an intermediately sized node that can work cooperatively with them to transmit data to the base station.

2.2.1) Mechanical Design:

- Enclosure: Must be minimum possible dimensions for portability.

2.2.2) Power System:

- Solar Panel (SP) Power: 500mW
- SP Voltage Range: 4 – 6.4V (4.8 nominal)
- Battery Type: NiMH, 3x1.2V, 2100mAH
- Battery Life: Completely sustained if panels receive 4 hours of equivalent full irradiation per day.

2.2.3) Material Design:

- Solar Panel: Flexible and lightweight in order to facilitate a “wearable” data collection node.

2.2.4) Electrical Design:

- Ability to transmit via wireless protocol 75m.

2.2.5) Radiation Design:

- Must be able to receive data from the sensing nodes within 2.5m minimum.

2.2.6) Economic/Ergonomic:

- Size/wiring must be small and unobtrusive to permit easy attachment to the outside of a spacesuit.

** The data node was not necessary in the final implementation.

2.3) Sensing Node:

The sensing node will contain the actual sensor(s). These will be made as small as possible to permit location in a wide variety of places, such as within areas of a spacesuit (i.e. within range of astronauts' core body heat) or on sensitive equipment. The sensing node will be capable of short distance communication, at least 2.5m to report data to a data node. Since the data node has increased power harvesting, it can facilitate transmission back to the base station at greater distances.

2.2.1) Mechanical Design:

See 2.2.4 (Interconnects) and 2.26 (profile).

2.2.2) Power System:

- Battery Type: LiMan, 3V, 1.2mAH, Button Style
- Battery Life: 9Hrs of normal operation

2.2.4) Electrical Design:

Note: NASA is most concerned with the implementation of the sensing network communications. For the purposes of developing a prototype, the parameter of interest for demonstration will be temperature.

- Temperature Range: -30° to 150° C
- Separate data analysis portion of PCB from sensors through interconnects so that nodes can be outfitted with other sensors for future upgradeability.

2.2.5) Radiation Design:

- Ability to report sensor data a minimum distance of 2.5m.

2.2.6) Economic/Ergonomic:

- Designed for minimum height profile to allow flexibility in placement.

3.0) Accepted Technical Design:

The following section outlines the implemented system. Figure [1] shows a block diagram of the entire system. Detailed explanations of each portion of the block diagram are covered in the following order:

- 3.1. Solar Panel Array and Control;
- 3.2. Power Supply and Battery Bank;
- 3.3. Base Station Communication and Interface; and
- 3.4. Sensor Node Operation.

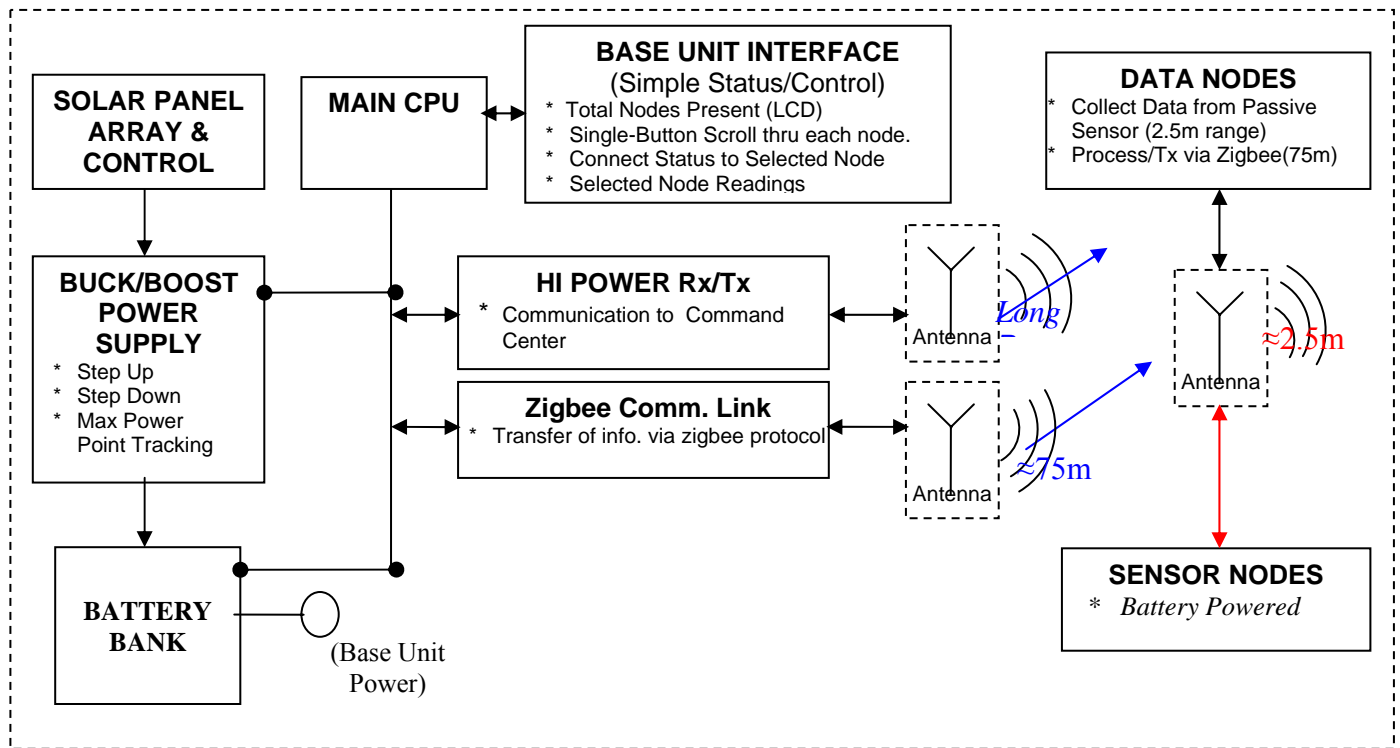


Figure 1: Detailed Block Diagram of System

3.1) Solar Panel Array and Control: (See Figure[18])

Author: Ben McDonald

3.1.1) Theoretical Advantage of Solar Tracking

Author: Josh Mahaffey

Before introducing the design aspects of a solar tracking mechanism, consider, first, the theoretical advantage of such a tracking scheme.

Most photovoltaic applications utilize harvested solar energy from a stationary solar panel; however, the novelty of this project lies in the ability to implement an algorithm that tracks the azimuthal position of the sun throughout a given period of sunshine. In order to quantitatively understand the advantages of this expanded capability, consider the following scenario: a solar panel is fixed at some elevation angle θ and azimuth ϕ as shown in figure [2]. The panel is oriented such that, at mid-day, the solar panel achieves maximum irradiation; however, at the beginning and end of a day it receives zero, and throughout the other periods, only a portion of the sun's radiated energy is incident on the panels

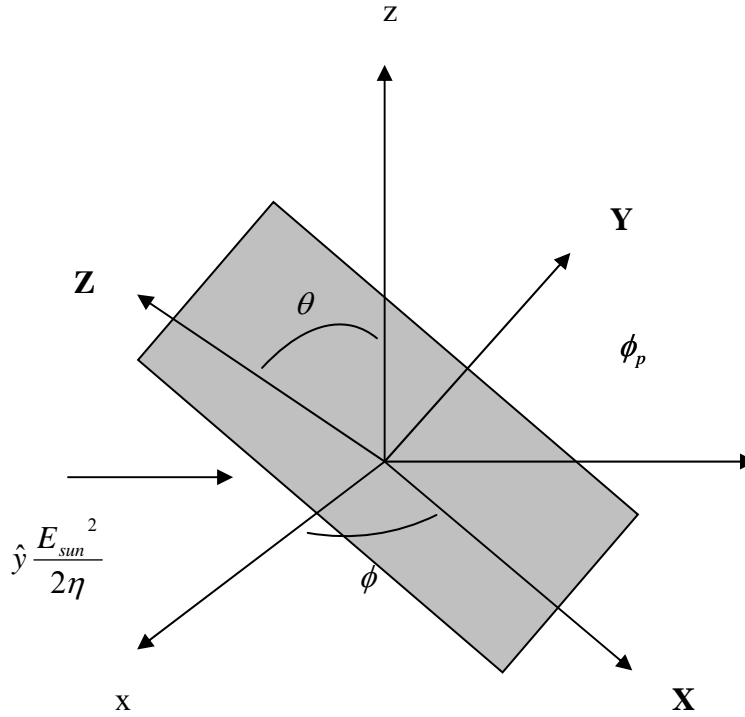


Figure 2: General Problem of Incident Power Density

Obtaining a relation for power density incident on the panels in relation to θ and ϕ using figure [2] is somewhat difficult to analyze. Therefore, in order to quantify this relation, one may transform the problem of figure [2] into a much simpler one by using Euler angles. The result of this transformation is that of figure [3]. One can see that after this relatively simple manipulation a direct relationship is obtained between

the azimuth and elevation with respect to the average power density that is incident on the panels. This relationship is given as

$$P_{avg} = \frac{E_{sun}^2}{2\eta} \iint \cos \theta_p \cos \phi_p dXdY \Rightarrow \frac{E_{sun}^2}{2\eta} LH \cos \theta_p \cos \phi_p [W] \quad [1]$$

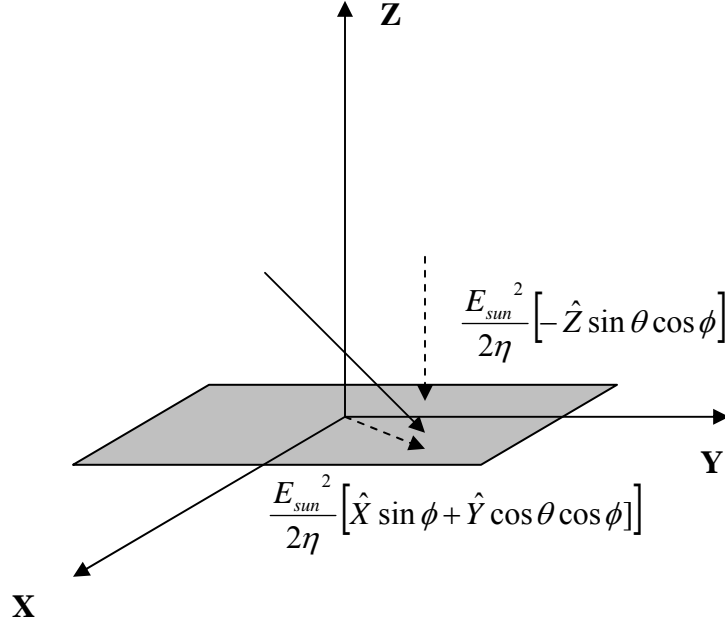


Figure 3: Transformed Problem of Incident Power Density

Utilizing equation [1], one may assume that the elevation is fixed at a position that optimizes the sun's output energy such that $\cos \theta = 1$. By tracking the sun's azimuthal position throughout a given day, it is assumed possible to receive 100% of the available radiation. This assumption, along with the equation derived above, yields the comparison plots shown in figure [4].

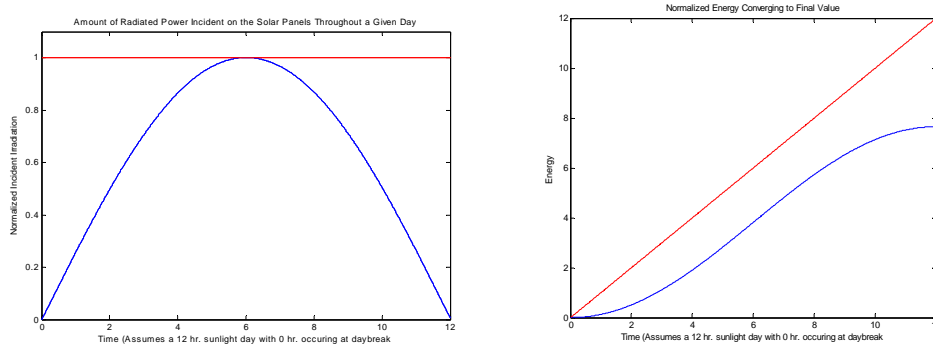


Figure 4: Incident Power Density and Energy Comparisons

From the figures above, it is apparent that the energy attained from a stationary panel would be less than 67% of the total energy attained by simply adding tracking capability to a solar system. This simple example demonstrates the the necessity of a proper algorithm and mechanical capability to track the positioning of the sun. For

this reason, having tracking capabilities is obviously a key criterion for the design of a system which is capable of maximizing the solar energy gain.

3.1.2) Overview of Solar Panel Tracking:

In this section, the method, mentioned in the theory above, of ensuring maximum energy harvesting is expanded to practicality.

After setting the solar panel at an optimum elevation angle, θ , based on the position of latitude, the azimuthal angle is tracked throughout a given solar day. In order to track the maximum intensity of the sun, the solar panels are used as more than an energy source; they are utilized as sensors to monitor the open circuit voltage (Voc). Based on the voltage changes, the panels are able to determine if the sun's position has shifted, and move to the new location. The circuit used to complete this task is below in figure[5]. The hardware and mechanical construction of the solar panel array is shown in figure [6]. Refer to the block diagram and module in figures [7] and table [1] for explicit functionality and electrical characteristics.

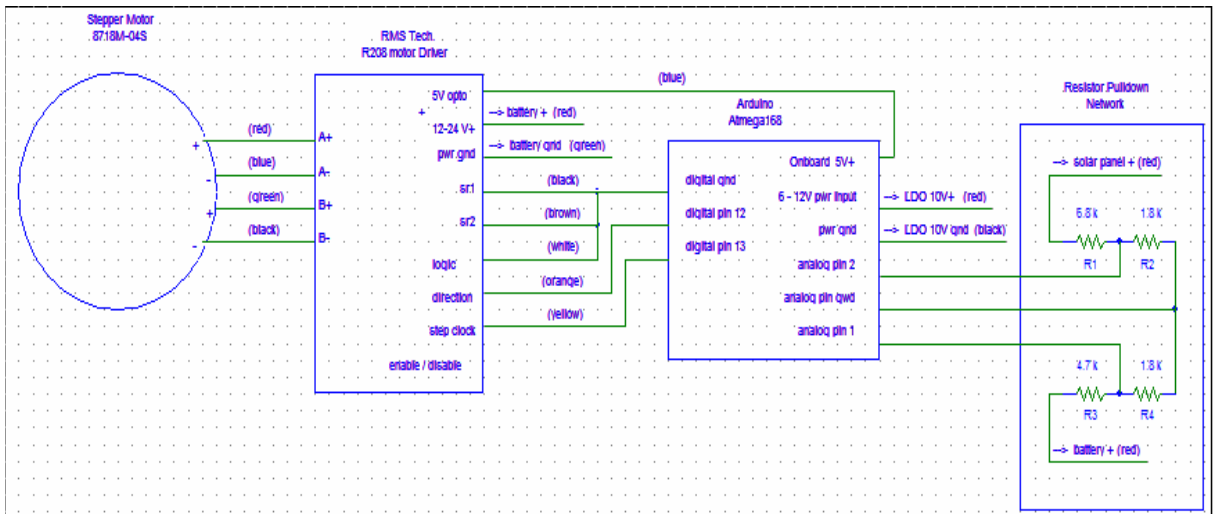


Figure 5: Solar Panel Array and Control Circuit

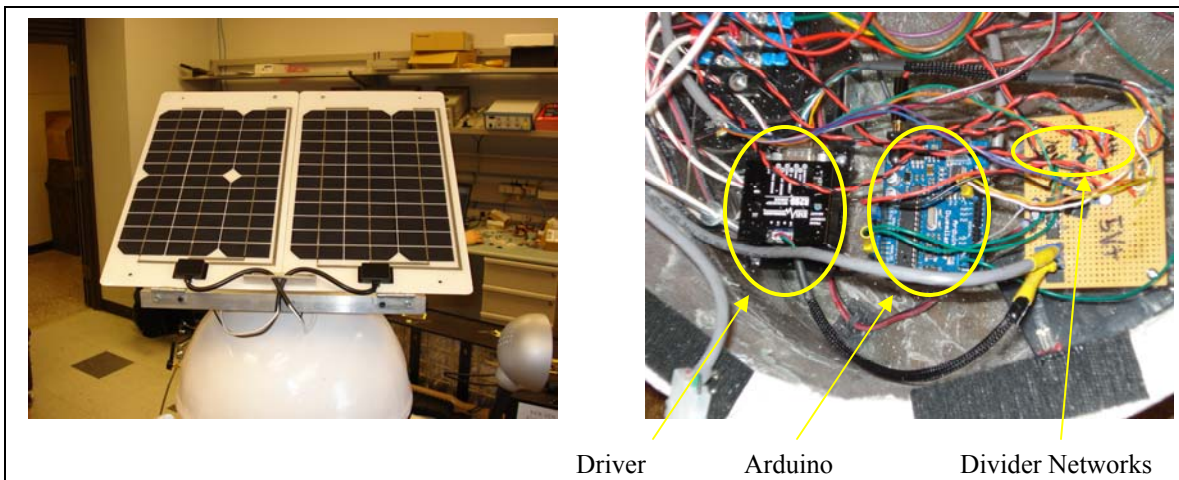


Figure 6: Solar Panel Array and Hardware Implementation

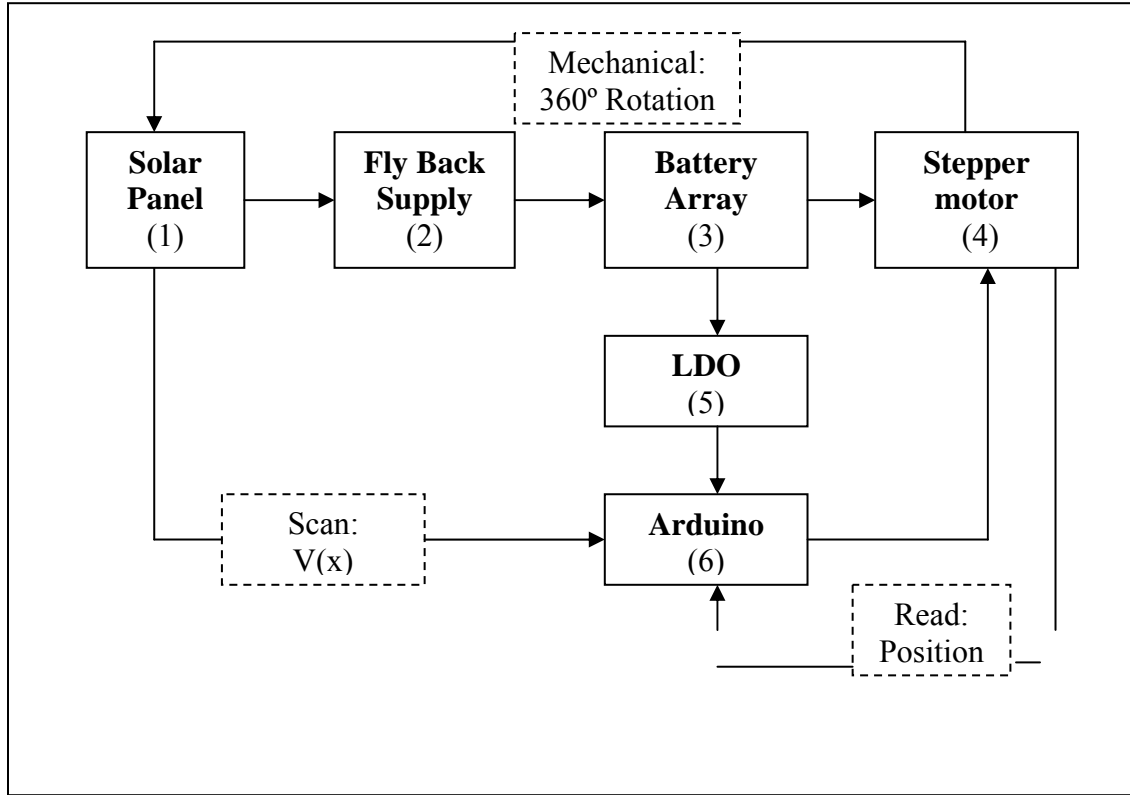


Figure 7: Solar Panel/stepper motor wiring and communication diagram with power supply.

Module	Solar Panel Array and Control Considerations				
Designer	Benjamin McDonald				
General Description	1) The solar panel(1) acts as a sensor outputting voltage readings to the Arduino(6).				
	2) The stepper motor(4) which is receiving position instruction for the Arduino(6) based on the voltage read from the solar panel				
	3) The Arduino(6) collect and track the scanned reading. Once finished with scan Arduino send position instruction to the stepper motor.				
	4) The LDO(5) supplies regulated voltage to the Arduino(6). The solar power is regulated by the Fly Back Supply(2) which recharges the battery(3) depleted power. The battery(5) power the stepper motor(4) directly.				
Solar Panels	The panels are required to generate 20 W. The solar panel will be mounted at an optimal angle based on the position of the light source.				
MCU	The Arduino draw less than 30mA.				
Stepper Motor	The stepper motor will be suitable for a downward force of 20lbs. Bipolar stepper motor to reverse directions when necessary.				
Electrical / Mechanical Considerations and Calculated Values		Min	Nominal	Max	Duty
Motor Ratings	torque		861.0oz-in		
	weight (solar panel array and mount)		approx. 15lbs		
	motor frequency (pwm)		10-hz	15-Hz	
	steps per revolution		200±02		
	degrees per step		1.8°		

Table 1: Solar Panel Array and Control Module.

3.1.3) Position Tracking Software

Figure [8] explains in the process of logic in the tracking control algorithm in the form of a flow graph, while figure [9] shows the pseudo-code implementation. Upon system start-up, the panels are rotated by the stepper motor 360 degrees (in 1.8 degree increments) and the voltages at each of the 200 positions are scaled by a resistive network and read into the arduino chip as depicted in figure [5]. The motor position of maximum open circuit voltage is stored into the arduino's memory; at the end of the 360 degree rotation, the panels shift back to the location of maximum irradiation (based on the open circuit voltage).

Since the sun is documented to move approximately 15 degrees per hour, the program's primary while loop occurs only after a thirty minute delay after locating the position of maximum open-circuit voltage. The panels will scan approximately 20° for each reading (10° to the left and the right of the current position), and rotate to the position where the maximum voltage was detected. Initially, wiring constraints were the reason for the three possible paths shown in the flow diagram of figure [8] (1. go to the maximum position; 2. rotate 360 degrees minus the maximum position; and 3. rotate 360 degrees plus the maximum position). In this manner, the panel will never rotate 180° in either direction, and the minimal wiring length could be calculated. However, a method was derived whereby very little solar panel wire is necessary, and there is no chance of the wire becoming entangled on any other part of the enclosure. This innovative solution will be introduced in appendix B. Although this methodology would allow the panels to track the position of the sun without the need for implementing the three options described above (eg. all that is necessary is to find the position of maximum voltage and direct the panels there), new code was not developed because of the last minute implementation of this new wiring system.

The final portion of the flow diagram and pseudo-code is for the saving of wasted power consumption. During dark hours, the panel voltage was observed to never exceed an open-circuit voltage of nearly 0.25 V of a maximum of 5.0 V. As a result, 0.25 V is considered the threshold "dark" voltage of the panels. If the voltage of the panels drops below this threshold for a pre-determined amount of time (in this case five minutes) the main loop will enter a 1 hour delay. Once the delay is entered, the voltage will be read periodically; however, if the panel voltage does not rise above 0.25 V during the "dark" delay, the program assumes that the panels, indeed, entered a period of no sunlight. On the other hand, if the reading is above the threshold, the code falls back into the main program loop. This serves as a "sanity check" for the program just in case the panels enter dark mode due to an anomaly other than darkness (eg. if someone stands in front of the panels). A counter is updated every hour for 10 hours (representing the ten hours of night); the program will fall back into the program loop once the counter is exceeded.

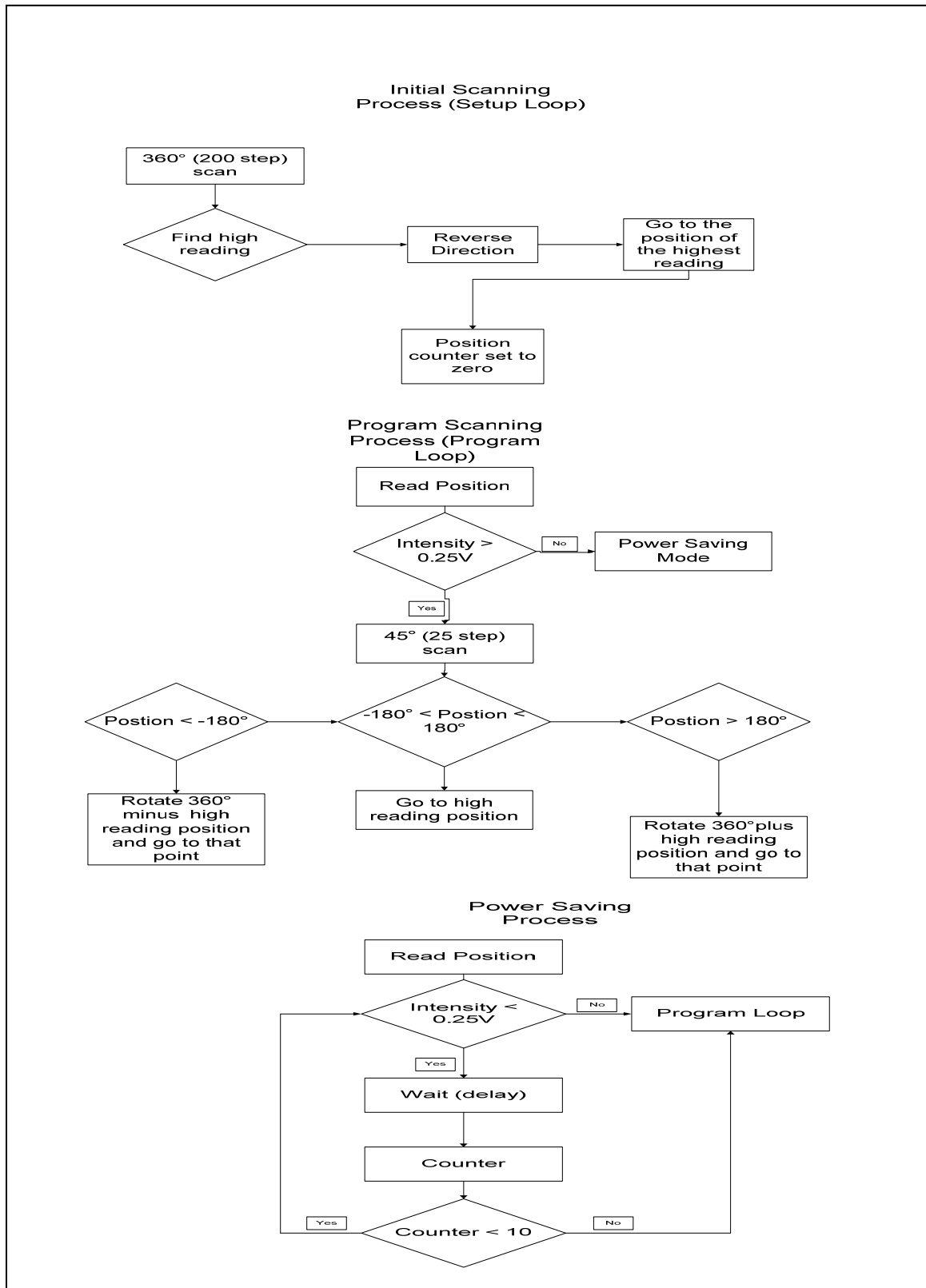


Figure 8: Solar Panel Array and Control Module Software Flow Diagram.

3.2) Flyback Power Supply & Battery Bank (See Figure[1])

Author: Jeff Petermann

The original design of the power supply called for a *buck-boost* topology. The most simply implemented version of this uses a single inductor, however it has the distinct drawback that the output is inverted. This was solved by using a coupled inductor, to correct for the inversion. Next, the turns ratio was adjusted to lower the peak input current. The system in its final implementation would be more aptly referred to as a discontinuous current mode (DCM) flyback.

The DCM mode allowed for easier implementation of Maximum Power Point Tracking Algorithm (MPP), to maximize the energy harvested by the system, by lowering the processing requirements (DCM impedance is not directly altered by the load). In addition, Flyback Power Supplies are capable of operating in both buck and boost so the output can be regulated to 14.2V from the 8-22V solar panel (photovoltaic module or PVM) input.

3.2.1) Detailed Block Diagram:

Figure[10] shows flyback converter with connections. Blocks with dashed lines indicate functions being performed, while solid lines indicate hardware/component blocks.

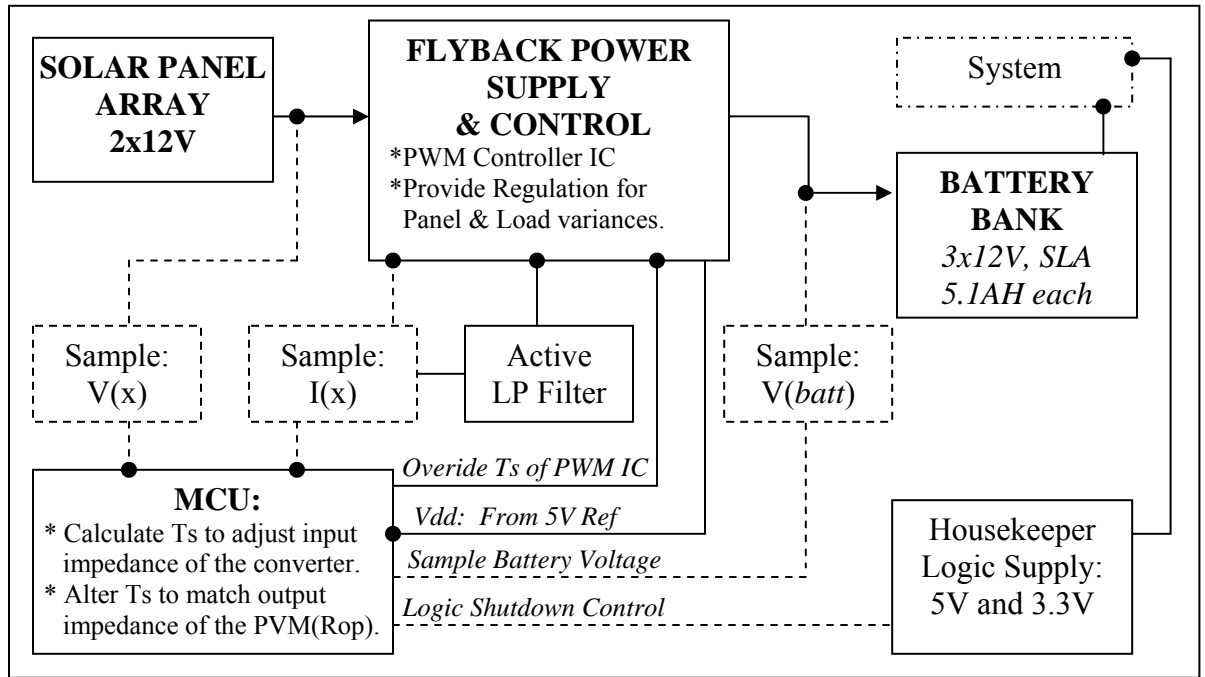


Figure 10: Block diagram of base station power unit.

3.2.2) DCM Flyback Relations

To permit rapid calculation of parameters, a Matlab script was used to take any necessary input specifications and estimate design parameters. The results of the simulation are shown in the Appendix using Matlab's publishing feature. In summary design relations were taken from [2] and are as follows:

Input Parmaters Required:

Minimum Expected Input Voltage
Maximum Expected Input Voltage
Voltage Rating of Switching Element
Desired Nominal Switching Frequency (3 can be simulated at once)
Voltage Output
Power Output
Al value of the core being used (H/N^2)
Core Effective Area

Steps/Equations:

- 1) Calculate a range of Turns Ratios based on Max FET Rating (2).
- 2) Calculate Ton for worst case input condition (3).
- 3) Calculate desired inductance (4).
- 4) Calculate peak current (5).
- 5) Calculate the required turns for a given core (6).
- 6) Calculate Peak Flux Density for the Core (7).

Note, that some energy relations are included in the simulation but do not apply to the results presented in this design. Lastly the required wire size is estimated by assuming that 500 circular mils / Ampere(RMS) is sufficient.

$$\frac{N_p}{N_s} = a = \frac{V_{switch-max} - V_{in-min}}{V_{out} + 1} \quad [2] \quad T_{on-max} = \frac{(V_{out} + 1) * \left(\frac{N_p}{N_s}\right) * (D_{Max-Duty} * T_s)}{(V_{in-min} - 1) + (V_{out} + 1) * \left(\frac{N_p}{N_s}\right)} \quad [5]$$

$$L_p = \frac{(V_{in-min} * T_{on})^2}{(2.5 * T_s * P_o)} \quad [3] \quad I_{pk} = \frac{V_{in-min} * T_{on}}{L_p} \quad [6]$$

$$N_p = 1000 * \sqrt{\frac{L_p}{N_s}} \quad N_s = \frac{N_p}{a} \quad [4] \quad B_{peak} = \frac{V_{in-min} * T_{on} * 10^8}{N_p * A_e} \quad [7]$$

3.2.3) Maximum Power Point Tracking (MPP):

Aside from the basic function of regulating 14.2V to the system batteries, the system implements a maximum power point tracking algorithm. The MCU (Atmel TINY13V, 8 bit) controls the switching period of the supply via it's PWM output. The TI PWM controller will adjust the on time(T_{on}) of the switching MOSFET (see schematic, Fig[15]) by comparing an error signal taken from the output to a fixed reference. This T_{on} is proportional to a peak input current for a given input voltage condition, and represents the energy required to maintain regulation.

Further, the MCU will adjust the PWM switching frequency (T_s) by increments of 1.67uS between the ranges of 16.67uS to 37.5uS. This corresponds to PWM

switching frequencies of 27-60KHz. This effectively changes the input impedance of the converter as demonstrated in [1]. The input power is estimated by the MCU through sampling of the voltage and peak current on a cycle-by-cycle basis. Subsequent cycles are compared to determine if the incremental adjustment resulted in an increase of input power or a decrease. If it has decreased, T_s will be incremented in the opposite direction. When the change in input power equals 0 ($dP=0$), then the maximum power point has been reached. At this condition $R_{op}=R_i$ and the optimal balance exists between T_{on} , T_s , and their relationship to the PVM conditions.

To demonstrate this graphically, Figure[11] shows the current, power, and output impedance (R_{op}) relationship versus voltage of a solar panel at typical conditions. This is the typical plot based upon the model presented in [1]. A Matlab script included in the appendix allows this curve to be simulated for varying conditions of power density and temperature. R_{op} is simply the V/I from the first curve and is considered the PVM's output impedance.

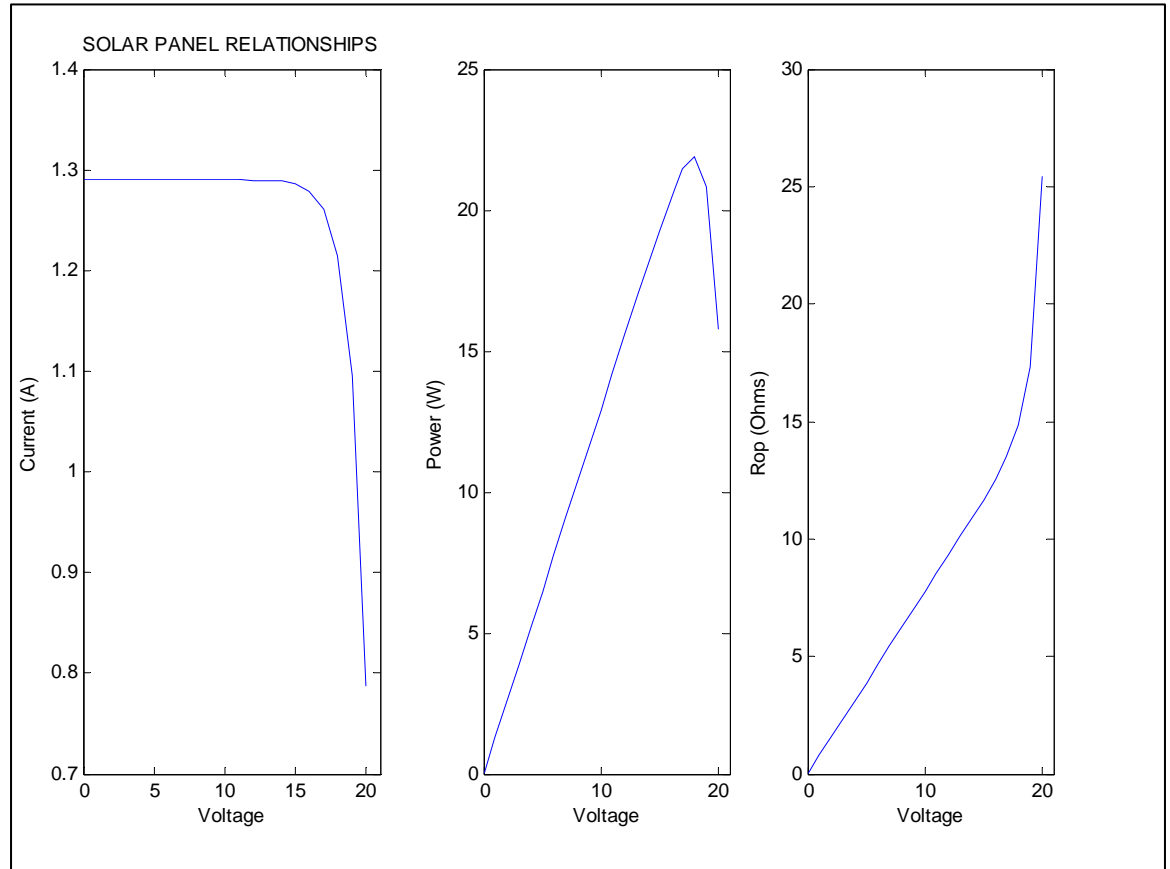


Figure 11: Solar Panel Model

The maximum duty cycle allowed by the PWM module of the MCU is 95% while the minimum is effectively 0. Varying load conditions will demand larger amounts of energy and hence longer T_{on} 's or higher duty cycles. Figure[12] demonstrates the theoretical capture range of input impedances for 3 duty cycles over the range of allowed T_s periods. The converter can match an impedance of 4.7 ohms. The typical solar panel depicted in figure[12] has in input voltage of 6V at this point which is

well below the panel's useable range. This demonstrates that system can take on an appropriate combination of duty cycle and T_s to match any typical load presented by a PVM module.

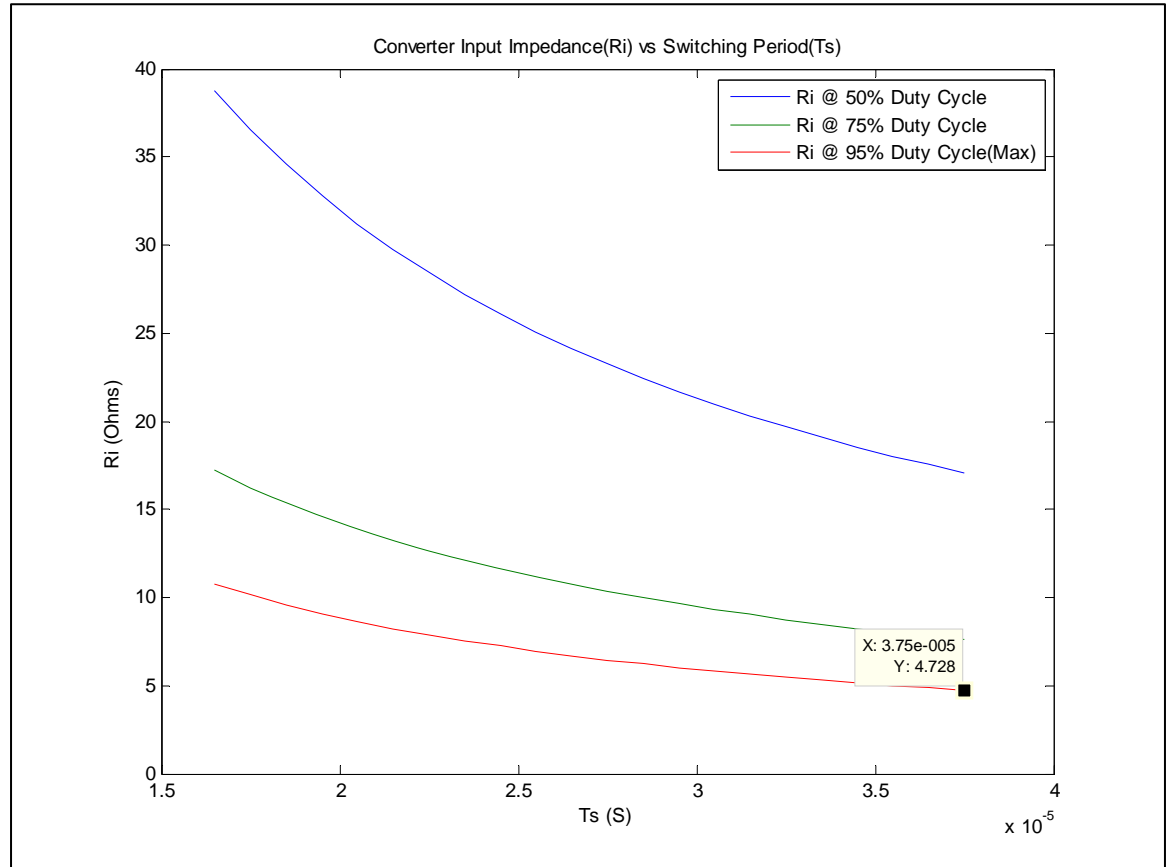


Figure 12: Converter Input Impedance as a function of T_s and Duty Cycle

3.2.4) Additional Features Available:

Added functionality can be implemented in the present PCB design through modification of the MCU's firmware. The battery voltage is connected to one of the AD channels via a resistor divider so the MCU can sample it. This could be potentially used to implement a charging cut-off at either the full or catastrophically low condition.

Also, there are two LDO's used to generate logic level voltages for the rest of the system. These devices are equipped with a shutdown feature which has been tied to the MCU I/O. To save power in an emergency battery situation, the logic in the base node could be put to sleep by the MCU.

3.2.5) Results and System Requirements:

Figure[13] shows the performance of the power supply over the range of 10-22V inputs. For comparison, these tests were run with and without the MPP algorithm implemented. The MPP is strictly implemented through software and can be

completely disabled in the MCU's code. When not in MPP mode, the power supply operates at a nominal PWM switching frequency of 29.9KHz.

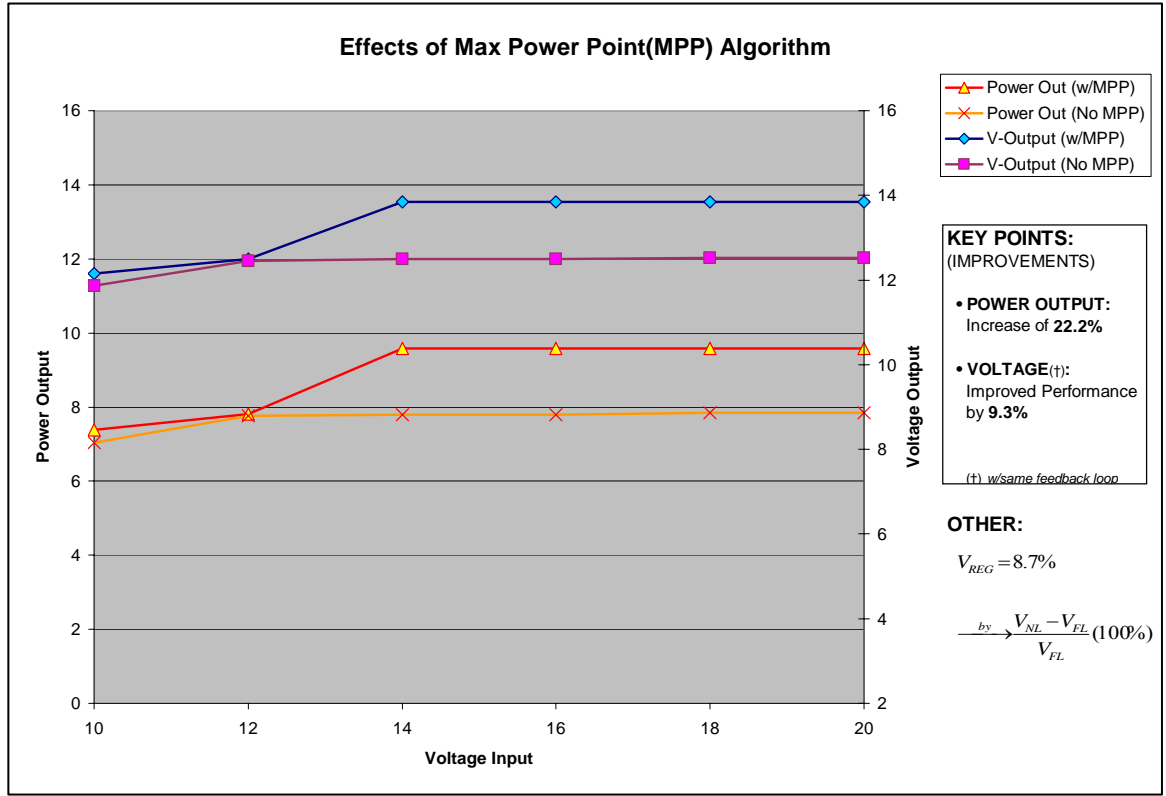


Figure 13: Converter Performance with Analysis of MPP Contribution

The MPP algorithm improved Full Load Voltage Regulation by 9.3% while increasing the power output of the system to 22.2% based on the range of operating supply voltages. Voltage regulation was a respectable 8.7% given the added capabilities of the converter.

The final power system requirements are shown in Table[2]. Average current consumption was determined using low-value current sense resistors in series with their respective major components. As an example, Figure[14] shows the average current draw of the base node communication module. For testing one transmission burst was measured, however the actual current draw was 14.2mA continuous plus the 2.28mS burst substituted into equation 8.

In addition, the complete schematic is shown in Figure[15] with accompanying costed bill of materials in Table[3]. A software block diagram is shown in Figure[18].

Module	Major Component	Sub Component	Sub Component Description	Current (avg)	Duty Cycle	Amp-Hours	Notes
Base Station	Solar Panel:			1.2	0.167	0.2	Based on 4 Equiv hours of full irradiation (Design Spec).
	Power Supply	Power Supply Losses:	Conversion Efficiency	-105.6E-3	1	-105.6E-3	Based on 15% Loss from Independent Tests of the converter.
		5V Output	MAX 232 (TTL side)	-1.0E-6	1	-1.0E-6	Handles PC interface
			LCD	-9.8E-3	1	-9.8E-3	
		3.3V Output	Zigbee Comm Chip and Main Processor	-14.6E-3	1	-14.6E-3	Implemented algorithm for Sun Position Tracker and handled CPU interface which simulated command center communications.
		Main Output:	Motor Driver Circuit	-10.0E-3	0.0417	-417.0E-6	15s every 6 minutes
			Arduino	-7.5E-3	1	-7.5E-3	Handles PC interface/Sun Position Tracking System.
			Max232 (UART, 0-10V)	-22.0E-3	1	-22.0E-3	Handles PC interface
			Batteries			15.3E+0	3x12V @ 5.1AH each. In parallel, total AH=15.3.
Base Station Summary	SUMMARY PARAMETERS: OVERALL LIFE OF SYSTEM					TOTALS	NOTES
	NORMAL DAY OF OPERATION: AH CONSUMPTION					160.0E-3	Total Draw of AH in one day of normal operation.
	NET ENERGY IN/OUT OF SYSTEM: 1 DAY					40.0E-3	System has replaced all drain from day's usage in 4H + 40mAH.
	MAXIMUM NUMBER OF DARK DAYS OPERATION (no PVM)					95.7	The system has overhead to cover a long-haul transmission system. Our specification was only 18 days.

Table 2: Distribution of Amp-Hour Usage for the Base Node.

$$I_{AVG} = I_1 \left(\frac{T_1}{T_S} \right) + I_2 \left(\frac{T_2}{T_S} \right) \quad [8]$$

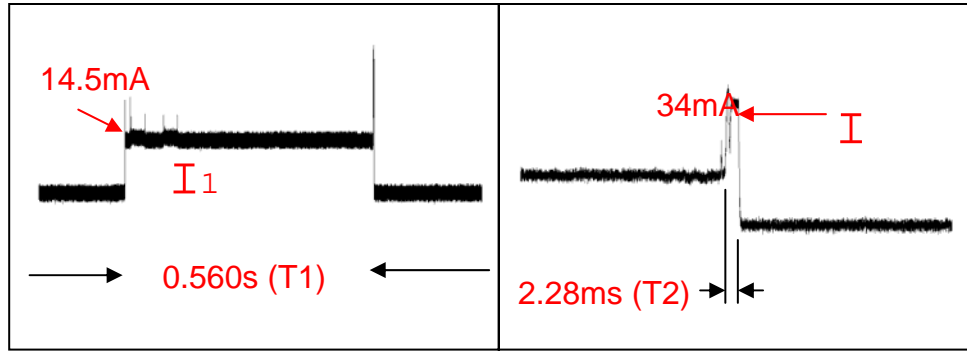


Figure 14: Average current measurement using sense resistor.

3.2.6) Future Work:

There are a couple of issues that can be improved upon for the future. First, the active filter section inverts the result which requires extra calculation time. The present version of this omits this section and the A/D is taken straight across the current sense resistor at a known interval. As a result, T_s tends to “dance” around the optimal point. The chief impediment lies in the fact that the MCU takes time consuming single ended conversions.

The system has been fully bench tested but due to time constraints, field tests were not completed. Additional long term tests would help to establish parameters mentioned in 3.2.4 to ensure battery health. The solar panel output current was lower than anticipated so the system relies upon an input capacitor to help supply the peak currents. The negative impacts of this need to be formalized. Possible solutions might be to operate the supply in continuous-mode (CM, versus DCM) which would limit the peak current requirements and/or improved solar panel specifications.

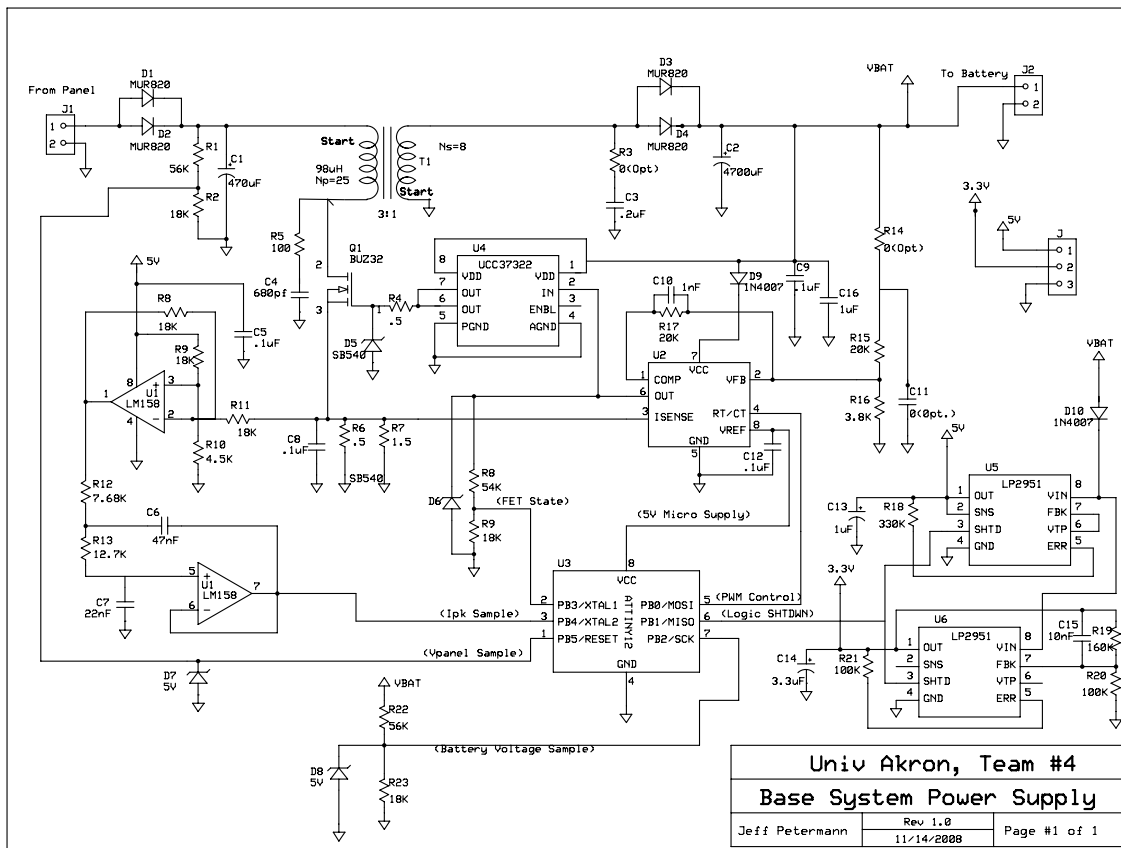


Figure 15: Power Converter Schematic

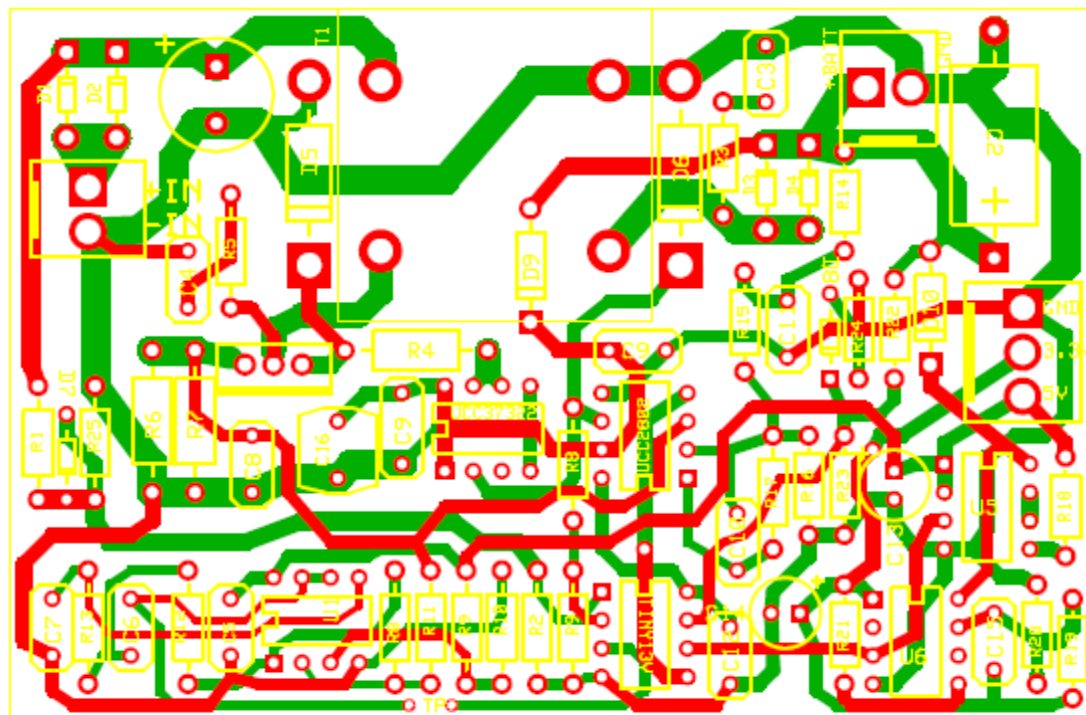


Figure 16: PCB Layout of the Base Station Power Supply

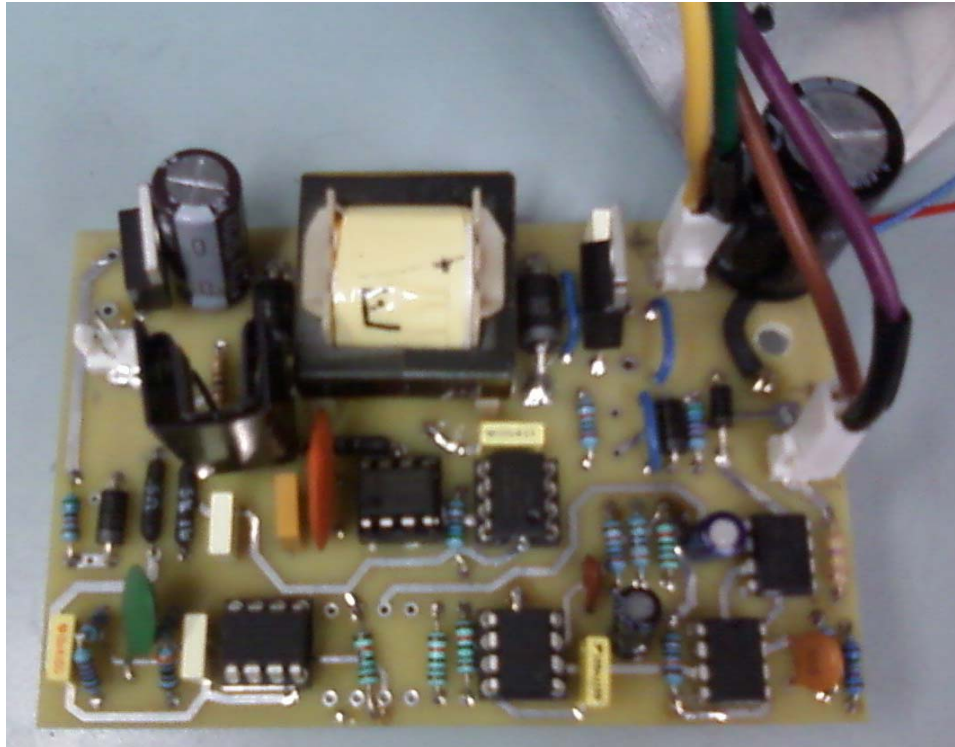


Figure 17: Actual Implementation of Flyback Power Supply

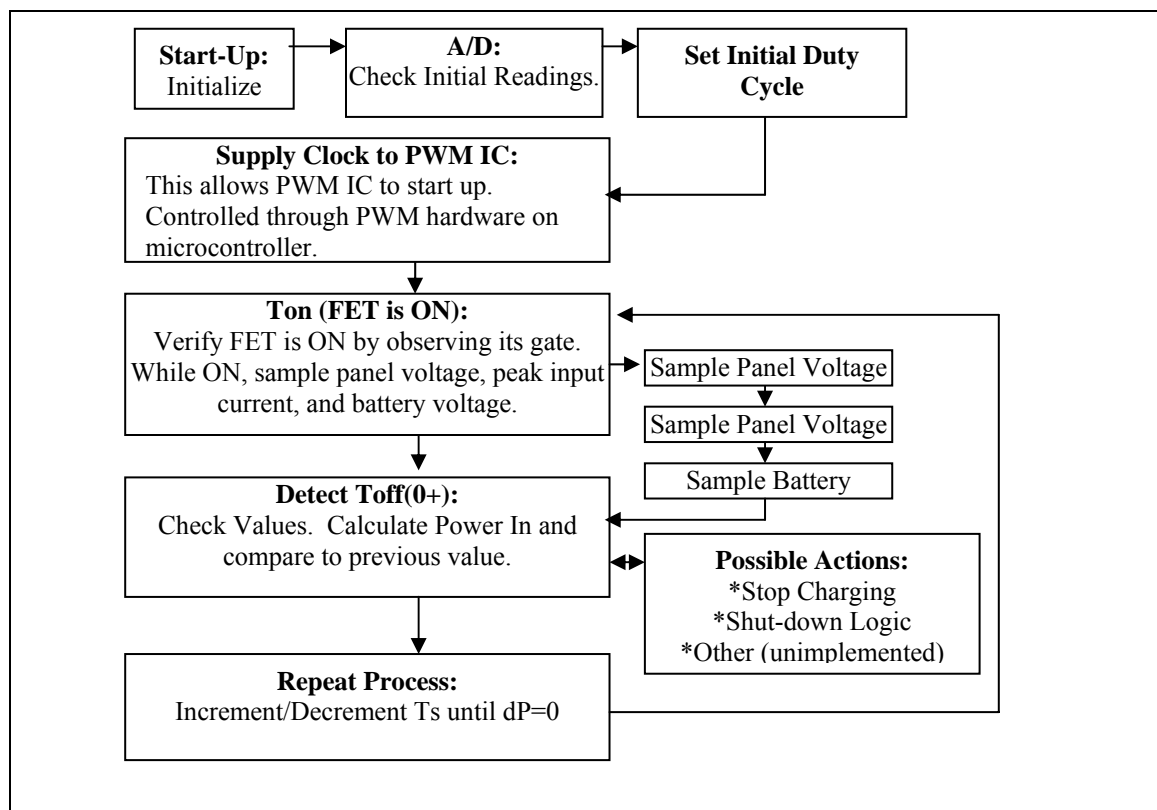


Figure 18: Software Block Diagram

REF DESIGNATOR	DESCRIPTION	QTY	\$\$/ea	\$\$/ext
C1	Capacitor, Al Electrolytic, 470uF, 35VDC	1	\$0.200	\$0.200
C2	Capacitor, Al Electrolytic, 4700uF, 79mOhm ESR, 25VDC	1	\$0.200	\$0.200
C3, C5, C8, C9, C12	Capacitor, Metal-Film, Box, .1uF, 50V	5	\$0.150	\$0.750
C4	Capacitor, Ceramic, 680pf, 100V	1	\$0.150	\$0.150
C6	Capacitor, Ceramic, 47nF 50V	1	\$0.150	\$0.150
C7	Capacitor, Ceramic, 22nF, 50V	1	\$0.150	\$0.150
C10	Capacitor, Ceramic, 1nF	1	\$0.150	\$0.150
C11	0(Opt), Could be used for feedback comp	1	\$0.000	\$0.000
C13	Capacitor, Ceramic, 1uF	1	\$0.150	\$0.150
C14	Capacitor, Al Electrolytic, 3.3uF, 25VDC	1	\$0.200	\$0.200
C15	Capacitor, Ceramic, 10nF	1	\$0.150	\$0.150
C16	Capacitor, Al Electrolytic, 1uF	1	\$0.200	\$0.200
D1,2,3,4	Ultra Fast Diode, MUR820, 8A, 200V	4	\$0.700	\$2.800
D5,D6	Schottky Diode, SB540, 5A, 40V	2	\$0.500	\$1.000
D7,D8	TVS, 5V Effective.	2	\$0.250	\$0.500
D9,D10	Diode, 1A, 1N4007	2	\$0.050	\$0.100
J1, J2	Molex, 2Pin	2	\$0.500	\$1.000
J3	Molex, 3Pin	1	\$0.500	\$0.500
Q1	Mosfet, 200V, 9.5A, N-Ch, BUZ32	1	\$1.450	\$1.450
R1	Resistor, .25W, 56K ohm	1	\$0.020	\$0.020
R2	Resistor, .25W, 18K, ohm	1	\$0.020	\$0.020
R3	0(Opt), Secondary Winding Snubber	1	\$0.000	\$0.000
R4, R6	Resistor, 1W, 0.5 ohm	2	\$0.700	\$1.400
R5	Resistor, .25W, 100 ohm	1	\$0.020	\$0.020
R7	Resistor, 1W, 1.5 ohm	1	\$0.700	\$0.700
R8, R22	Resistor, .25W, 56K ohm	2	\$0.020	\$0.040
R8(2), R9, R11, R23	Resistor, .25W, 18K ohm	4	\$0.020	\$0.080
R10	Resistor, .25W, 4.5K ohm	1	\$0.020	\$0.020
R12	Resistor, .25W, 7.68K ohm	1	\$0.020	\$0.020
R13	Resistor, .25W, 12.7K ohm	1	\$0.020	\$0.020
R14	0(Opt), Could be used for feedback comp	1	\$0.000	\$0.000
R15, R17	Resistor, .25W, 20K ohm	2	\$0.020	\$0.040
R16	Resistor, .25W, 3.8K ohm	1	\$0.020	\$0.020
R18	Resistor, .25W, 330K ohm	1	\$0.020	\$0.020
R19	Resistor, .25W, 160K ohm	1	\$0.020	\$0.020
R20,R21	Resistor, .25W, 100K ohm	2	\$0.020	\$0.040
T1	Custom, Np=25, Ns=8, Nycera, EE25, Al=160mH	1	\$1.000	\$1.000
U1	Dual Op Amp, LM158	1	\$0.250	\$0.250
U2	TI Switching Regulator, UCC28C40	1	\$1.800	\$1.800
U3	MCU, 8 bit, ATTINY13V	1	\$0.650	\$0.650
U4	UCC37322 Mosfet Driver IC, CMOS	1	\$1.330	\$1.330
U5,U6	LP2951, LDO Regulator, Adjustable, CMOS	2	\$0.600	\$1.200
FAB	CUSTOM PCB, Express PCB	1	\$17.000	\$17.000
TOTAL COST				\$35.510

Table 3: Costed Bill of Materials

[1]Ortiz-Rivera, Eduardo, "Maximum Power Point Tracking Using the Optimal Duty Ratio for DC-DC Converters and Load Matching in Photovoltaic Applications", Applied Power, Electronics Conference and Exposition, 2008

[2] Pressman, Abraham I, "Switching Power Supply Design", McGraw Hill, 1998

3.3) Base Station Communications and Interfacing Software (See Figure[23])

Author: Jacob Pozderac and Josh Mahaffey

The Zigbee communications protocol has been implemented in our system using Texas Instrument's open-source code, SimpliciTI. This small-scale Zigbee protocol is capable of implementing up to eight different communications link that connect directly to a single data hub (i.e. base station). Each of the Zigbee data frames must be transmitted with a preamble sequence, addressing information, post script sequence, and have handshaking capabilities (see figure [19] displaying the standard communication frame for Zigbee transmission); these are addressed directly by SimpliciTI utilizing a set of pre-defined functions to establish a network and perform data transmission. The only requirement that must be handled directly by the programmer is creating the functionality to build and decode the frame payload (i.e. transmitted message).

			Frame Field	Data count	Address Info	Frame Payload	Frame Check
			MAC Header		MAC Payload		MAC Footer
Preamble Sequence	Start of Frame Del	Frame Length	MAC Protocol Data Unit (MPDU)				

Figure 19: MAC Protocol Implemented in Each Data Transmission

The software at the base unit must be capable of receiving and filtering link requests, obtaining data from the linked sensor units, and displaying the information on an LCD; these are described below:

1. Recognition of Link Request and Network Establishment
 - a. A link request issued by the sensor nodes as described in section 3.4 must be discernable by a specific link token. Upon recognition of this pre-determined link token, the base unit issues a join message that contains a link id. The join message is received by the issuing sensor unit alone, and the link id is stored in the sensor node memory and sent during each transmission frame.
2. Obtaining and Processing Sensor Data
 - a. Utilizing the receive function supplied by the SimpliciTI protocol, frames from each node in the network enter the receive buffer at the base node; these frames are processed on a first in first out (FIFO) basis. During processing, all of the preamble and addressing information depicted in figure 16 are neglected, simply leaving the message data to be read and stored. This data is gathered with and stored and the unsigned 8 bit integers (i.e. the message data as required by SimpliciTI) is recombined to obtain the 32 bit pressure and 16 bit temperature data.

3. Displaying Information

- a. Upon initialization of the base node communication, the UART peripherals are configured and prepared to use for data transmission from the CC2430 buffer to an LCD. Upon reception of sensor node information, the pressure and/or temperature is converted from data bytes to character strings and displayed on an LCD.

From these requirements, the flow diagram and pseudo-code were developed; these are shown below in figures [20] through [22].

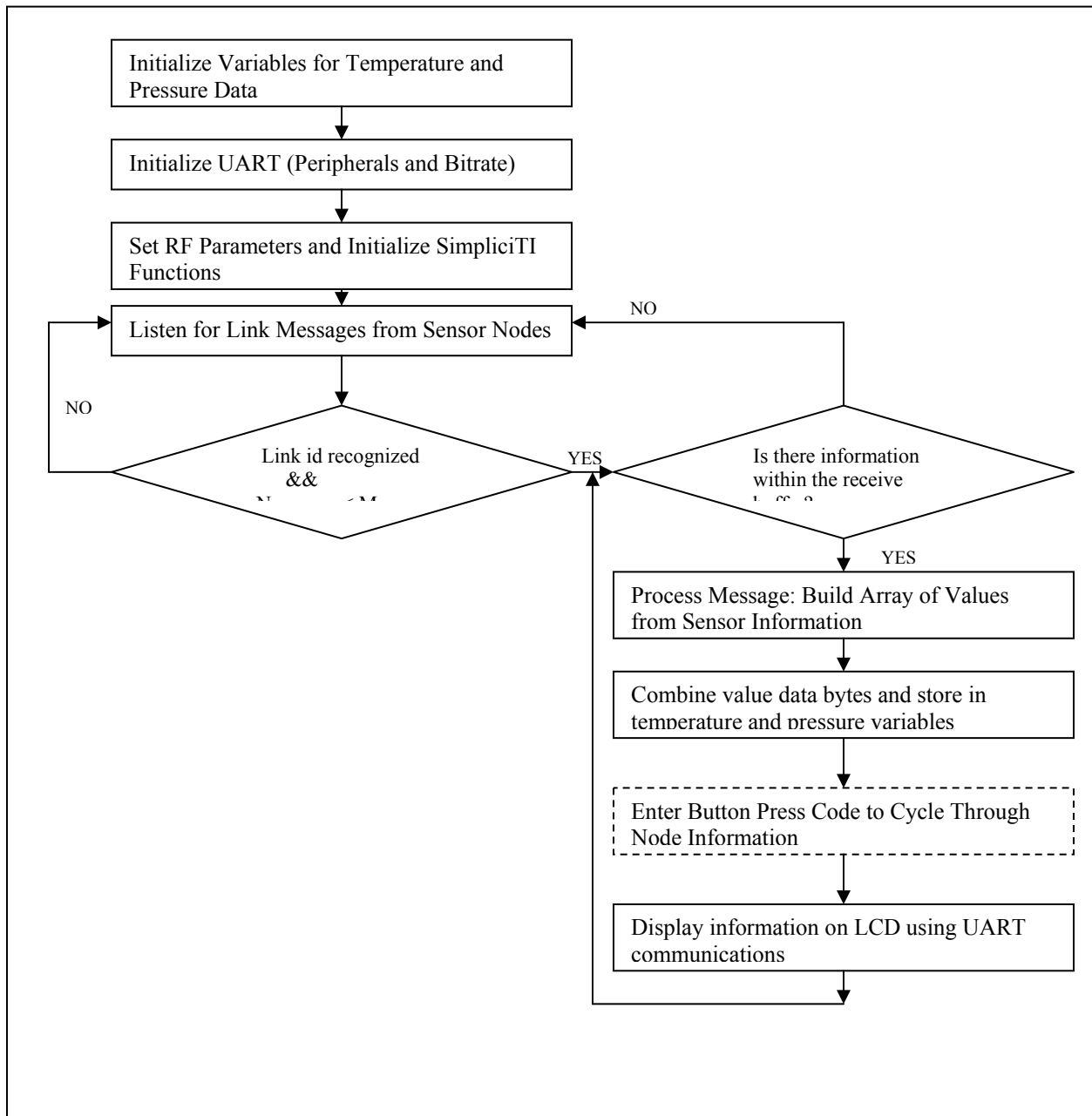


Figure 20: Base Station Communications Flow Diagram

Base Unit Pseudo-code

```

Include Functions;
Global Variable Defns;
Function Prototypes;

void main(void) {

    uint16_t temperature, temp_pressure, sign_test;
    uint32_t pressure;
    float temperature_float, pressure_float;

    init_SimpliciTI_radio();           // Initialize the base unit simpliciTI defined radio functions
    init_UART();                       // Initialize UART peripherals and bitrate (base node comm. – UART)

    init_network();                   // Initializes the network settings (link token, linkid, join token, etc)
    // The base node now recognizes what token id's it is looking for

    while(1)                          // Base node forever loop
    {
        while(1)                      // Listen for peers to join network
        {
            if (link_msg_received && num_peers <= max_no_peers) break;
        }
        num_peers++;

        if (msg_buffer)               // Is there any information in the receive buffer
        {
            uint8_t    msg[MAX_BUFFER_RECEIVE], len, i;

            /* process all frames within buffer */
            for (i = 0; i <= num_peers; i++)
            {
                if (msg_received(LID[i], msg, &len))    // is there a message from the current link id
                {
                    process_message(LID[i], msg, len);

                    /* Recombine the temperature information */
                    temperature = Value[1];             // Value array is created in process message
                                                         // sub-routine
                    temperature <<= 8;                  // Value[1] upper byte of temperature
                    temperature |= Value[2];            // Value[2] lower byte of temperature
                    sign_test = temperature & 0x2000;    // Is the temperature a negative number
                    if (!sign_test)
                        temperature_float = (float)temperature/20;
                    else {
                        // Conversion for negative temperatures
                        temperature ^= 0x3FFF;
                        temperature += 1;
                        temperature_float = -((float)temperature)/20;
                    }
                    /* Recombine pressure data for calculation */
                    pressure = Value[3];                // Value[3,4,&5] are the pressure bytes
                    pressure <<= 16;                    // from MSB to LSB
                    temp_pressure = Value[4];
                    temp_pressure <<= 8;
                    temp_pressure |= Value[5];
                    pressure |= temp_pressure;
                    pressure_float = (float)pressure/4;

                    if (identifier_1) uart0send(name_1); // Look at the identifier byte to determine
                    elseif (identifier_2) uart0send(name_2); // which sensor node sent info.

                    uart0sendString(temperature, pressure, etc);
                    msg_buffer—
                }
            }
        }
    }
}

```

Figure 21: Base Station Communications Pseudo-code

One critical aspect of the pseudo-code shown in figure [21] is the ability to decode a message sent from each sensor node; these messages contain an array of unsigned 8 bit integers which are stored in a receive buffer upon reception. The pseudo-code shown in figure [22] addresses the message processing capabilities.

```
void process_message(uint8_t lid, uint8_t *msg, uint8_t len)
{
    if (len)                // Make sure that we are invoking the process message sub-routine
    {
        // because a message is in the buffer
        identifier = *msg;
        for(int i = 1; i <= MAX_BUFFER_RECEIVE; i++){ // Process entire message (message limited to buffer size)
            if(*(msg+i) == 0xFF){ // Stop byte sent at end of transmission
                Length = i-1;
                break;
            }
            Value[i] = *(msg+i); // Create an array of values populated by the transmitted messages
        }
        *msg |= NWK_APP_REPLY_BIT; // Replace message in buffer with acknowledge message
        SMPL_Send(lid, msg, len); // Send acknowledge frame back to the sender (sensor node)
    }
    return;
}
```

Figure 22: Process Message Pseudo-code

3.4) Sensing Node (See Figure[25])

Author: Josh Mahaffey

It has been determined that the best sensor node implementation is one that has low powered sensing capabilities and is outfitted with a rechargeable battery and small solar cell will suffice. In order to adhere to the requirements of an ultra-low powered sensor node, the electronics on board must be capable of operating under “sleep-mode” conditions (i.e. the quiescent current of the electronics must be in the low micro-amps in between sensor reads and transmissions). Figure [23] depicts the block diagram required to realize the sensor network. Also, a corresponding module is shown in table [4]; this briefly summarizes the component selections and electrical characteristics of the node.

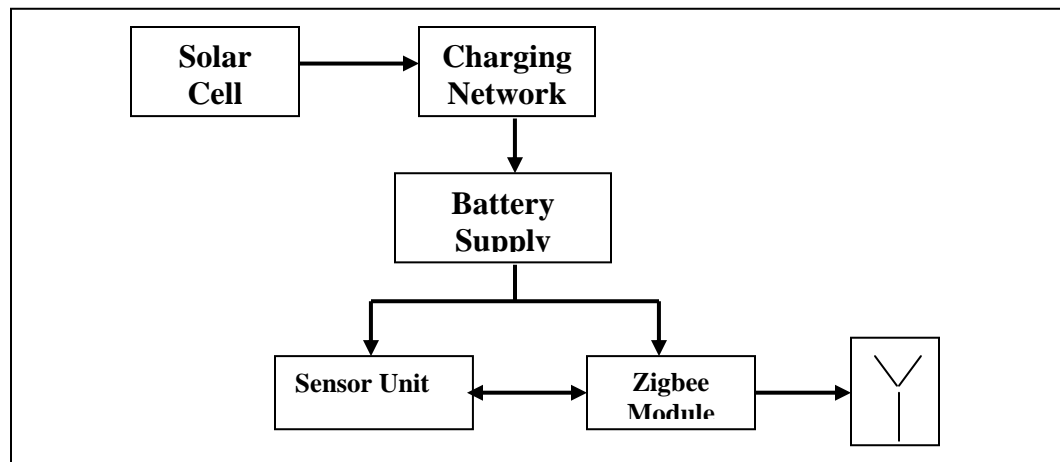


Figure 23: Overall sensing circuit block diagram with power supply.

Module	Sensor Node					
Designer	Josh Mahaffey					
System Components						
Solar Panel	PowerFilm 4.2 V, 22 mA solar cell. The dimensions are 1.5" X 3.5 "					
Charging Circuit	Adjustable LDO regulator circuit with output voltage of 3.2 V					
Batteries	LiMg 3.0 V 40 mAh batteries connected in parallel					
Sensor Unit	SCP 1000 dual temperature/ pressure sensor (see electrical characteristics below)					
Zigbee Module	CC2430EMK - TI's communications evaluation module					
Electrical Considerations and Calculated Values			Min	Nominal	Max	AH(1hr)
Inputs	Solar Cell Voltage [V]			4.2V		
	Battery Voltage [V]			3 V		
	Battery AH Capacity			4.00E-02		
	Current Supplied by Solar Cells [A]			2.20E-02		
System Draw	Zigbee Chip: Low current draw for short distance signal transmission [A]			3.40E-02		6.89E-07
	Sensors: (Temperature & Pressure) [A]			1.40E-02		2.77E-04
Hours Operation Without Sunligh (No Recharging)						5.30E-06
Total AH Draw: 24 Hours: (No Recharging)						1.07E-01
Hours Operation Without Sunlight (No Recharging)						9.00E+00
AH Replaced to system (Assume 4 Hr of full radiation)						1.40E-02

Table 4: Sensing Node Module

The block diagram shown above was utilized for each of the sensor nodes. Also, the sensor nodes were kept to a minimal number, two, simply to minimize cost. However, it should be noted that, for the communications protocol that was utilized, one could easily integrate up to eight different wireless sensing applications in the network.

3.4.1) Implementation of Sensor Node Hardware

The components that were utilized to actualize the diagram shown in figure [23] consist of the following:

1. Solar Cell
 - a. The solar cell, made by PowerFilm, has an operating voltage of 4.2 V and is capable of supplying 22 mA. It has a minimal face area of 3.5" X 1.5" and is flexible.
2. Battery
 - a. The battery was a LiMg button style battery rated at 3.0 V and 40 mAh. In order to increase the battery current capability, two batteries were connected in parallel for the final design.
3. Charging Circuit
 - a. Based on the recommendation from the battery vendor, a linear drop-out regulator was used to drop the panel voltage from the nominal 4.2 V to 3.2 V. The output of the regulator is then connected directly to the LiMg batteries (there is no need to utilize a trickle charging scheme for these particular batteries).

4. Sensing Unit

- a. The sensing unit that was realized was the SCP1000 by VTI industries; it is a dual temperature and pressure sensor that has the following characteristics:
 - i. Pressure Range: 30kPa to 120kPa (1 atm = 101 kPa)
 - ii. Temperature Range: -30C to +85C
 - iii. Supply Voltage: 2.2 V – 3.3 V
 - iv. Resolution: up to 19 bits (14 bits for dual temperature sensor)
 - v. Accuracy: +/- 0.15 kPa
 - vi. Current Consumption: < 25 uA.
- b. The above characteristics are what the data sheet provides; however, by cycling between sleep and operation modes, it is possible to obtain an average current consumption below 5 uA, thereby conserving battery life drastically.

5. Communication Module

- a. Texas Instrument's CC2430 evaluation modules were utilized for data transmission. These modules were used for several reasons:
 - i. a development kit was readily available for programming and testing;
 - ii. a matching network, antenna, and other necessary circuitry already existed on a single board with the CC2430 chip;
 - iii. the module has a very low quiescent current draw while the MCU and data transmission are inactive (0.5 uA).
- b. The zigbee protocol was actualized by using an open source code available from TI called SimpliciTI. This particular code had readily available functions to allow for multi-node communications by developing the necessary preamble and addressing information required for each data transmission.

The overall schematic of the sensor node is shown in figure [24] below, while each of the major system components are highlighted in table [5]. The part, description, and cost is covered in the table as well. Also shown below is the PCB design layout that was utilized for the implementation of the hardware components. After the design was verified and sent to be manufactured, a few flaws were noted:

1. the input to the voltage regulator was from the battery and not from a panel;
2. the output of the regulator was not connected to the battery terminal; and
3. a switch was left out of the design so that the quiescent current draw was constant.

Upon obtaining the PCBs, these mistakes were addressed and the PCB was modified accordingly. The final assembly consisting of all hardware is shown below in figure [25].

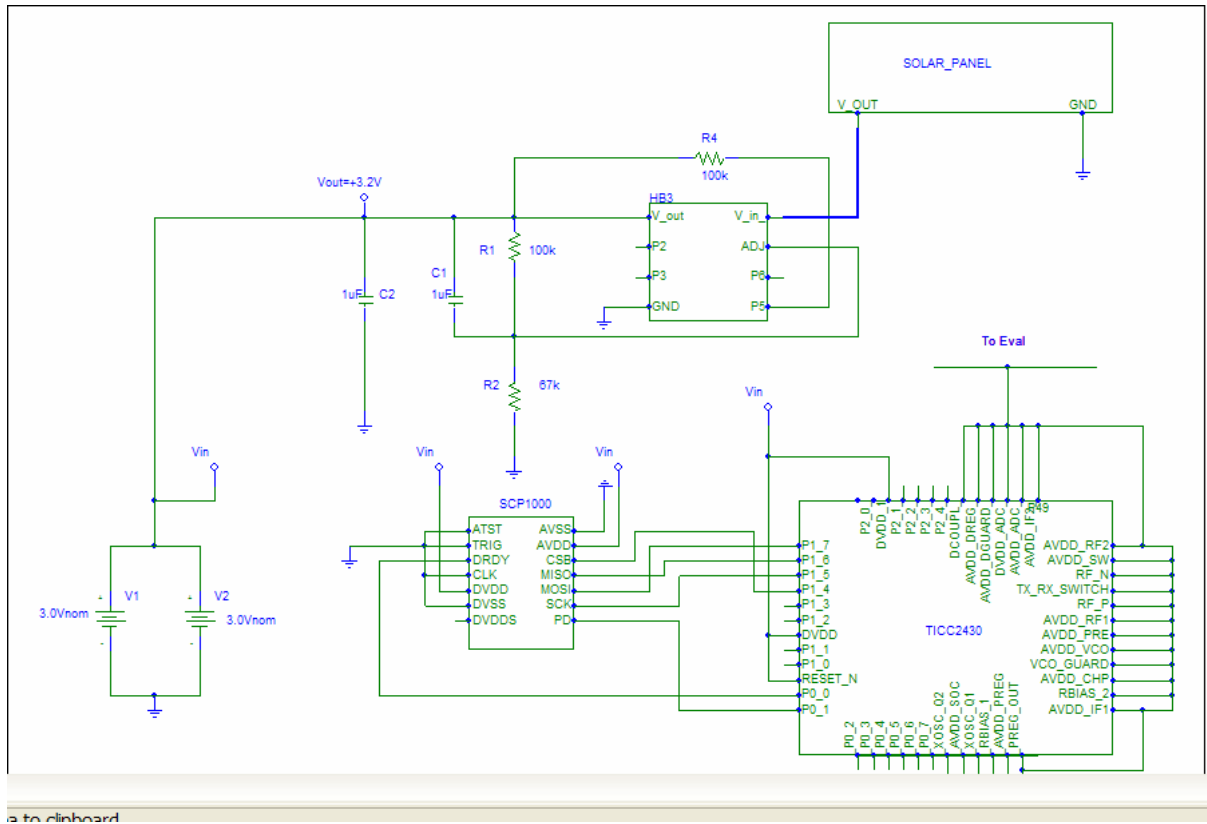


Figure 24: Overall Circuit Schematic For the Sensor Nodes

Sensor Node (Major Component) Hardware Parts List		
Part	Description	Cost
CC2430EMK	TI's communications evaluation module	\$50.00
SCP1000	VTI's combined pressure/temperature sensor	\$57.08
LDO	Microchipt adjustable drop-out regulator	\$0.42
SP4.2-37	PowerFilm 4.2 V, 22 mA solar panel	\$5.00
ML2020	Magenese Lithium battery rated for 3.0 V at 40 mAh	\$2.68

Table 5: Sensor Node Hardware Parts List

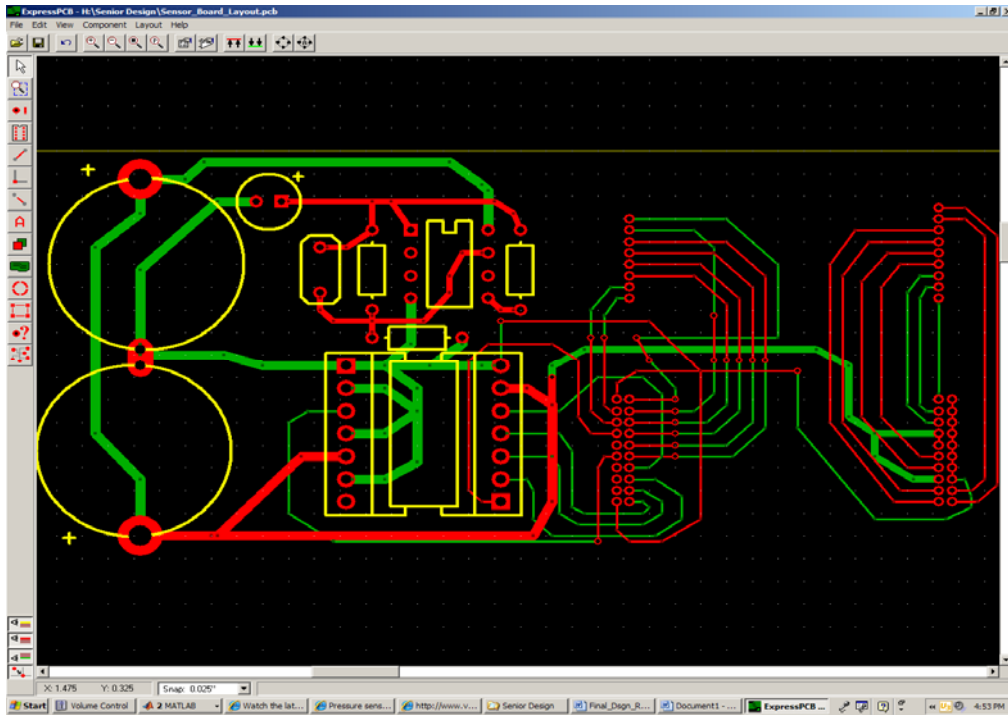


Figure 25: PCB layout of the sensor node board.

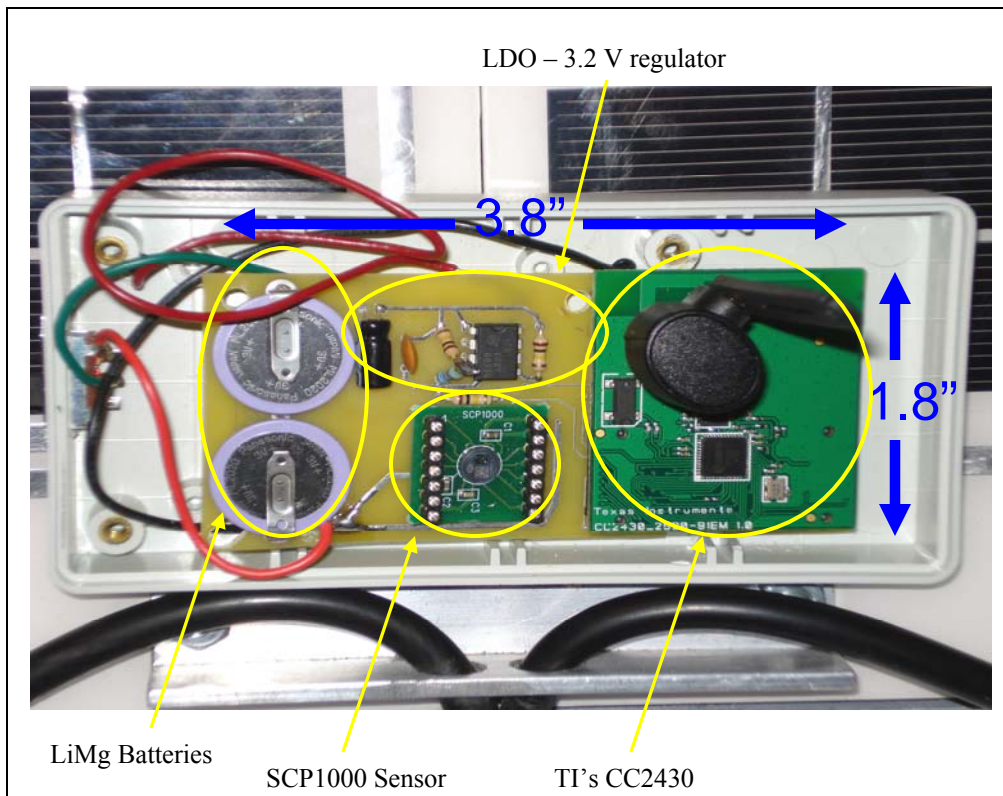


Figure 26: Picture of the Hardware at the Sensor Node (Note: the solar panel is not pictured, but lies on the opposite side of the circuitry).

3.4.2) Sensing Node and Communications Software

The main MCU at the sensor node exists within the CC2430 communication module. It is responsible for controlling all of the RF peripherals as well as interfacing with the SCP1000 via SPI in order to collect the sensor's information. The software has three important functions: 1. set the proper output power; 2. read data from the sensing unit; and 3. build a Zigbee communication frame.

3.4.2.1) Proper Output Power Setting

One of the RF peripherals that can be manipulated via software and is of large concern in this application is the output power. This setting determines the distance that the sensors are capable of communicating and has a large impact on the total current draw of the system. Using the well known Friis transmission equation

$$\frac{P_r}{P_t} = \frac{\lambda^2}{(4\pi R)^2} D_t D_r \quad [9]$$

the required transmission power can be determined keeping in mind that the required transmission distance is between 75m – 100m. Using $R = 100m$, $P_r = -94dBm$ (minimum detectable power by the receiver for the CC2430), and assuming that each antenna is a matched half-wavelength dipole

$$P_t = \frac{-2.981E-13[W]}{(0.125m)^2 (1.643)^2} = -40dBm. \quad [10]$$

This equation, however, neglects losses due to mismatch and EMI issues. Therefore, it was determined that an absolutely safe transmission power is approximately 0 dBm. Further testing proved that this setting is sufficient (transmission distance was approximately 100 yards) and the current draw is minimal.

3.4.2.2) Sensor Node Access

This relatively simple task is easily explained by viewing the flow graph and pseudo-code below.

3.4.2.3) Zigbee Frame

In order to adhere to the Zigbee protocol each data frame to be transmitted must contain the information shown in figure 19. As addressed in section 3.3, this is accomplished primarily by utilizing TI's SimplicTI protocol. Each frame contains the necessary preamble and post-scripting.

3.4.2.4) Flow Diagram and Pseudo-code

The communication module will operate cyclically in the following manner: 1. wake; 2. read; 3. transmit; and 4. sleep. However, before enter a state of continuously reading, transmitting, and waiting, the CC2430 I/O pins must be configured and the network established. The flow graph of figure [27] depicts the required code.

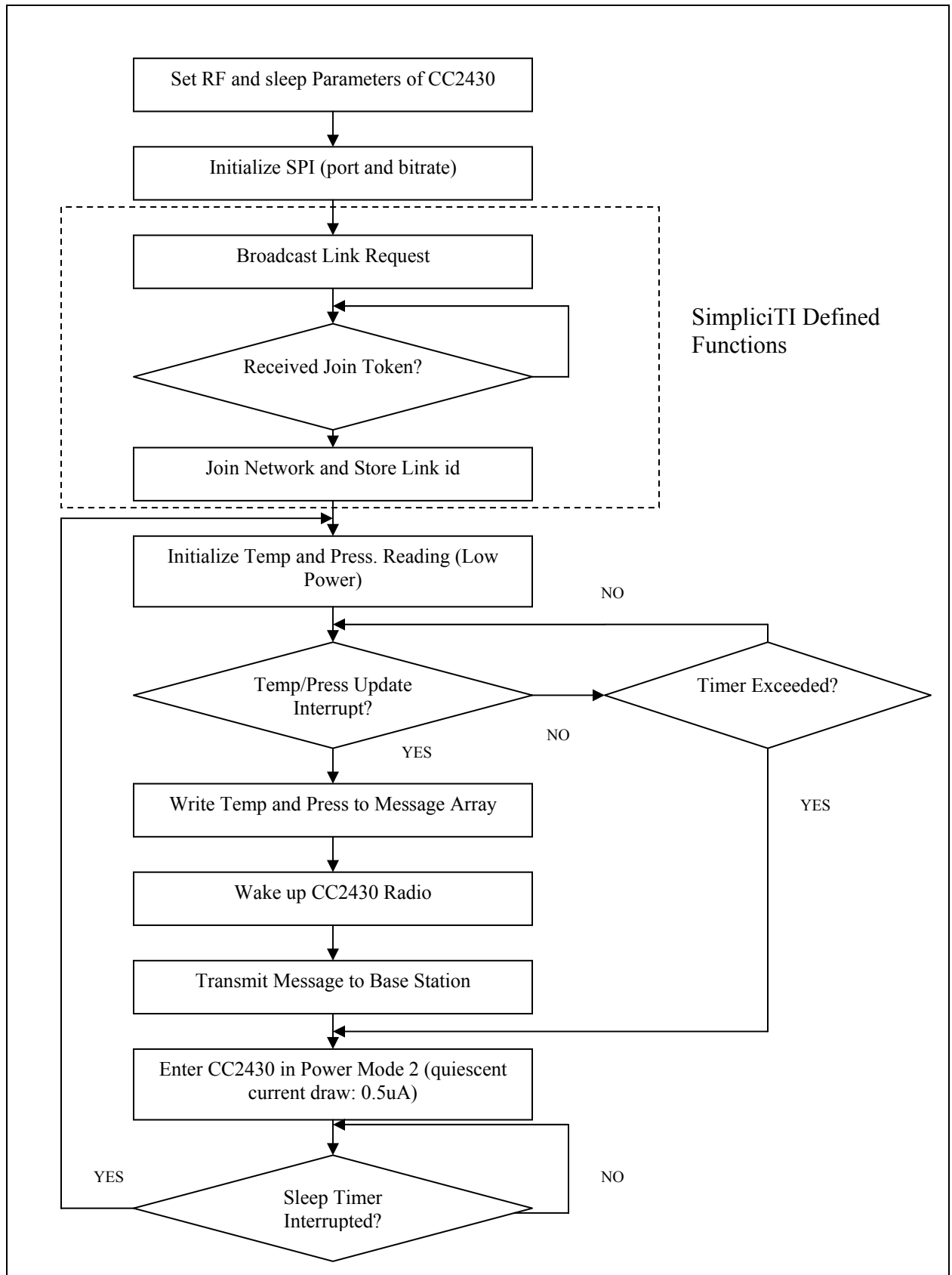


Figure 27: Software Flow Diagram for Sensor Nodes

From the above flow graph, it is possible to develop the required pseudo-code to implement sensor readings and transmission. Within the main body of the code are several sub-routines that are required to be defined upon implementation. The basic scheme of the code is the following:

1. Declare variables for sensor data;
2. Initialize SimpliciTI functions (add function for dBm setting) and SPI peripherals;
3. Read data from the sensor and store in the defined location;
4. Separate the 16 bit information into unsigned 8 bit integers;
5. Build a message;
6. Transmit; and
7. Sleep.

```

Sensor unit pseudo-code:

Include statements;

Prototype external functions;

main{
    uint16_t pressure_msb, pressure_lsb, temperature_data;
        // Storage location for sensor information
    uint8_t sensor_data[SENSOR_OUTPUT_LENGTH+1];
        // Message array is unsigned 8 bit integers. This is how we store the sensor // information after readout.
    sleep_bit_setting();           // Set compare values on the sleep timer
    init_SimpliciTI_radio();       // Initialize the simpliciTI functions
    init_SPI();                    // Initialize SPI comm. and pins

    link();                        // Broadcast a link transmission

    while (!join()) asm("NOP");    // Join the network that recognized the link

    while(1){                      // Forever Loop – Never need to rejoin a network

        init_sensor_read();
        if(DRDY_wait(time_to_wait)){
            // Get the sensor data
            pressure_msb = Read_Register(pressure_msb, number_of_bytes);
            pressure_lsb = Read_Register(pressure_lsb, number_of_bytes);
            temperature_data = Read_Register(temperature, number of bytes);

            sensor_data[1] = temperature_data >> 8;
            sensor_data[2] = temperature_data;
            sensor_data[3] = pressure_msb & 0x07;
            sensor_data[4] = pressure_lsb >> 8;
            sensor_data[5] = pressure_lsb;

            // Convert to unsigned 8 bit ints.

        }

        wake_radio();
        msg[0] = identifier;        // identifier bit – msg is the transmit variable
        msg[6] = stop_bit;
        for(int i = 1; i <= SENSOR_OUTPUT_LENGTH; i++)
            msg[i] = sensor_data[i];
        send_msg();
        radio_periph_sleep();
    } }

```

Figure 28: Pseudo-code for Sensor Node Software

3.4.3) Validation of CC2430 and SCP 1000 Software Interface

Before implementing the sensor nodes in the network hierarchy, the validity of the code had to be verified. According to the SCP1000 datasheet, in low power mode the MISO initializes the sensor to begin reading. After a successful read has occurred, the DRDY interrupt pin becomes a high logic and the sensor is capable of being read. Shown in figure [29] is a scope capture of the CC2430 pins that have been configured to obtain sensor information. Although a figure of the data capture is not shown (the display no longer reads properly), an LCD was initially connected to the CC2430's configured UART pin in order to verify the accuracy of the sensor. By placing the sensor under various temperature conditions (the barometric pressure cannot be varied) and comparing it the Fluke thermistor reading, it was determined that the temperature sensor updated the appropriate values during each read.

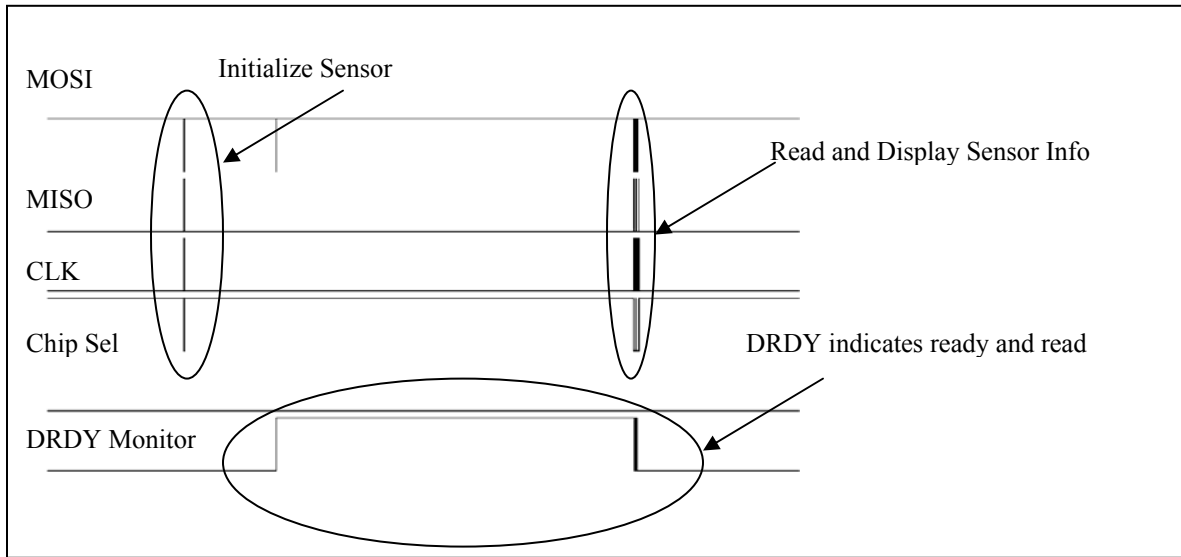


Figure 29: SPI and GPIO Output of CC2430 and Sensor

3.4.4) Sensor Node Current Profile

After implementing the hardware and software, a current profile was obtained in order to ascertain the drain of the system on the batteries. At the current dBm setting (as discussed previously, the maximum 0dBm setting is being utilized for maximum transmission distance), the total drain from the sensor node is 14.5mA for 560 ms and 34mA for approximately 2.28ms as depicted in figure [30]. Based on the specification listed in section 1, the battery life is required to be approximately 9 hours without irradiating the solar panels for any period of the day. In order to calculate the duty cycle required, consider

$$I_{avg} T_{cycle} = \frac{AH_{batt}}{T_{spec}} T_{cycle} = I_1 T_1 + I_2 T_2$$

where I_1 , T_1 , I_2 , and T_2 refer to the current consumptions shown in the figure [30] a and b respectively. Solving for T_{cycle} yields

$$T_{cycle} = \frac{14.5mA \times 0.560s + 34mA \times 0.00248s}{8.89mA} = 0.9229s .$$

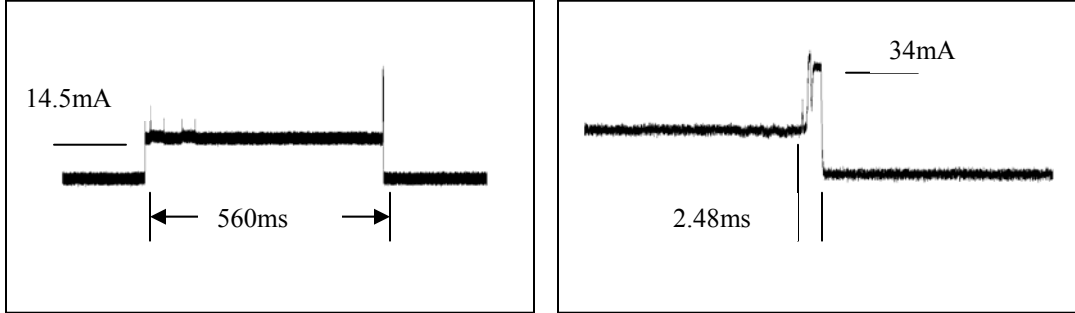


Figure 30: Current Consumption Profile of the Sensor Nodes

Using the equations above, it is also possible to plot the life cycle of the battery for varying duty cycles, T_{cycle} . The profile is shown in figure 28 below. The obvious conclusion that can be drawn from these observations is that by choosing an appropriate duty cycle, the lifetime of the batteries may be conserved for any required amount of time. Therefore, in applications where the measurand (quantity being sensed) is not critical and varies slowly as a function of time, T_{cycle} can be changed to minutes (or hours) and the battery life conserved greatly. However, for critical applications (i.e. monitoring various vital signs, detecting mission critical anomalies, etc.), the duty cycle must be chosen such that all impulsive events can be captured.

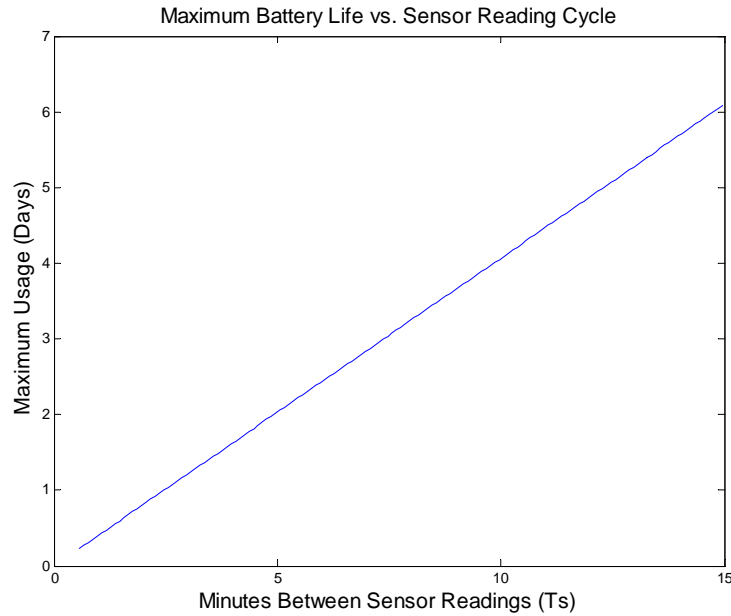


Figure 31: Battery Life Profile for Various Cycle Times

4.0) Service/Maintenance Instructions & Operations Manual

General

The following figure identifies the major components of the prototype unit. The batteries rest inside the outer fiberglass shell and are wired in parallel. There are three threaded stand-offs that hold the Plexiglas PCB fixing plate. All of the electronic components are mounded on this plate. The motor, power switch, and antenna are located in the top half of the prototype. Some of the main components are pictured separately in figure [33].

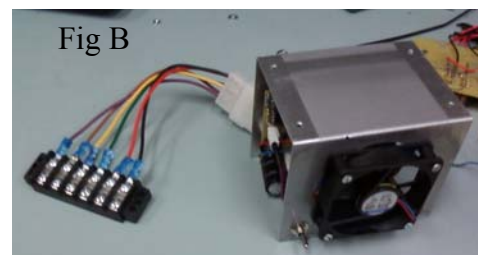
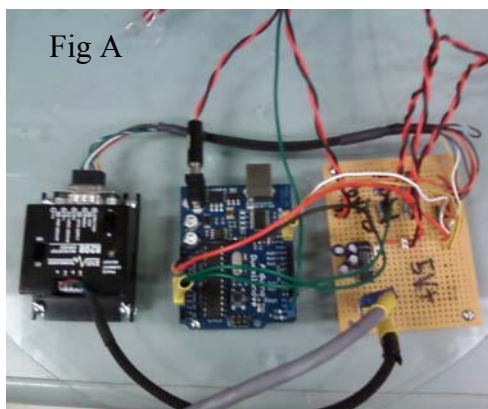
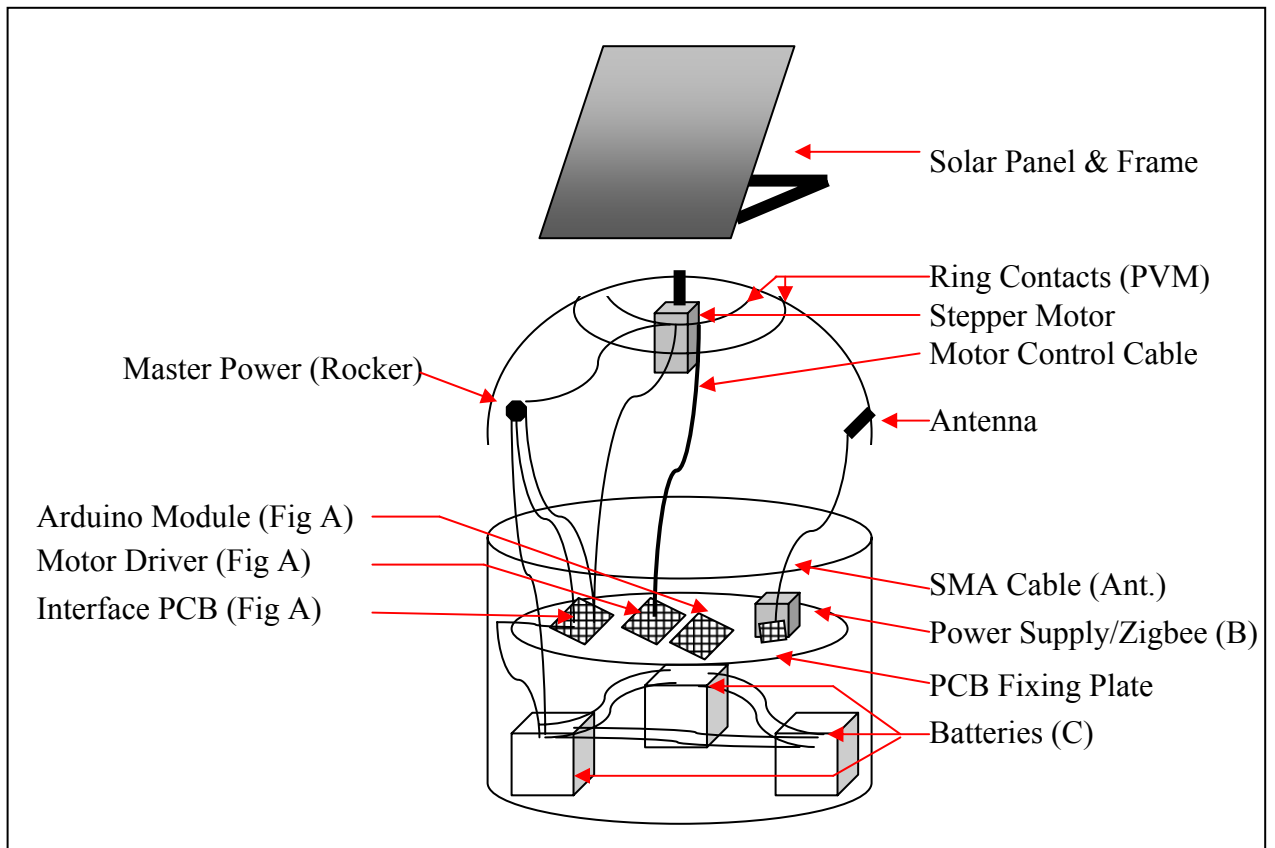


Figure 32: Assembly Diagrams and Photographs.

To disassemble the unit:

- 1) **WIRING:** For the purpose of prototyping, the top half is not fixed to the bottom half. However to remove the top half, the antenna must be unscrewed from the outside and allowed to pull away from the inside. The switch wires use female disconnects while an inline plastic connector houses the motor control wires.
- 2) **ELECTRONICS:** All electronics are housed on the Plexiglas PCB fixing plate. To remove this plate, 3 hex nuts must be removed from the threaded stand-offs.
- 3) **METAL HOUSING:** The metal housing shields the communications circuitry and general processing from the power converter unit. Figure [33] shows in further detail, except that the Zigbee module is not shown in the photo. To remove the electronics, remove the four screws on top of the metal enclosure and disconnect the in-line wire harness. The inner piece of the metal enclosure slides out.

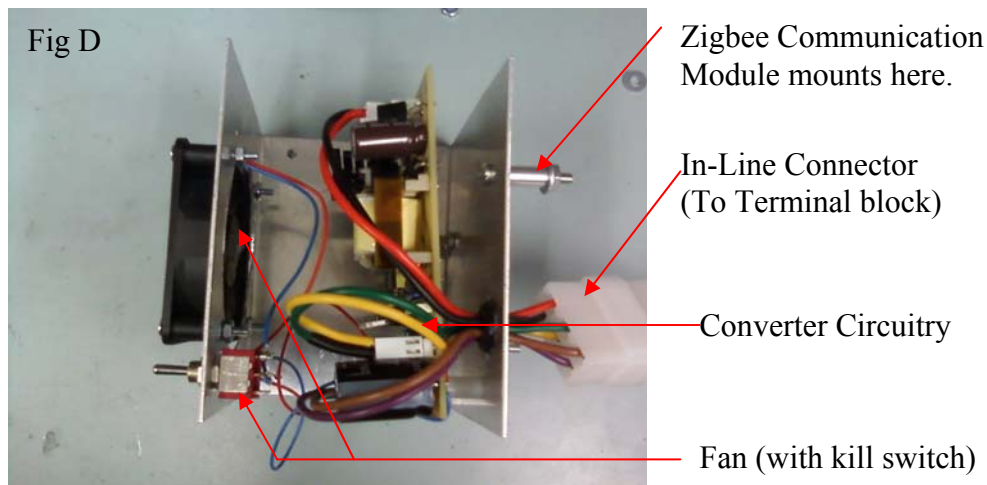


Figure 33: Power Supply Mount and Enclosure

Special Considerations & Cautions:

- 1) **BATTERIES:** The 12V Batteries used for this project are capable of delivering large amounts of currents. Shorting out these batteries will MELT WIRES! When servicing the sensor scavenging unit, always disconnect the batteries from the circuit by removing the +lead from the batteries to the rocker switch.
- 2) **ARDUINO MODULE:** The flash program memory of the Arduino Module can be reprogrammed via USB cable. However, when doing this make sure that the DC power in to the module is disconnected.
- 3) **OTHER FIRMWARE:** Atmel Tiny 13V MCU that controls the power supply is placed in an 8-Pin socket for easy removal. It was programmed with an STK500 development kit, IAR systems compiler, and AVR Studio 4. The other MCU functions utilize the built in 8 bit processor of the TI Zigbee modules. These were programmed via IAR Systems as well and the TI development kit.
- 4) **POWER-UP/VOLTAGE PROTECTION:** The inputs to the power supply are overvoltage and reverse-hookup protected however good practice would be to always connect battery power first, before connecting the power from the solar panels. This ensures all components are properly biased. Following the

connections in the following diagram will ensure that proper supply is provided to all other functional blocks.

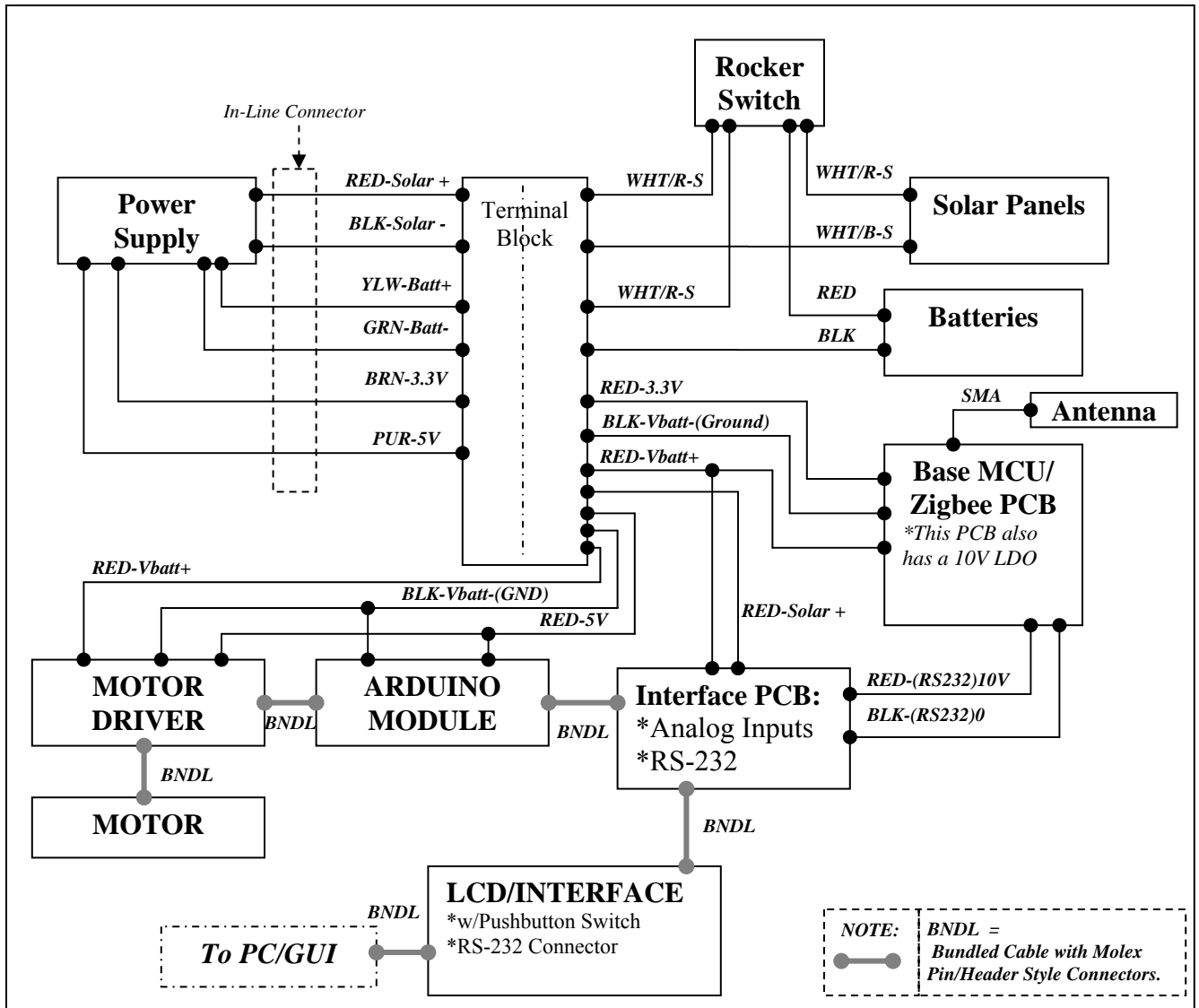


Figure 34: Block Diagram Showing Wired Connections

4.1) OPERATION NOTES:

Solar Position Tracker: When initially turning on the unit, a 360 degree scan will commence in which the unit locates the “hot-spot” position (largest measured open circuit voltage of the panel). Once this position is found, the panel will rotate to this position (after the full 360 degrees). Next, it will double check conditions within a 45 degree slice at a duty cycle set by software. Six minutes would be a typical duty cycle in actual operation. In this manner it will always ensure that the panel is oriented towards the sun’s position.

Zigbee Modules: After power up, the base node will attempt to locate any sensor nodes within the area. For a sensor node to be picked up, its slider switch must be moved to the “ON” position. Once detected, it will then “Link” and information

can be exchanged. The sensor nodes' transmitting duty cycle can be set to establish any mix of battery life/data rate desired. At other times, the sensor node will enter sleep mode to conserve battery power. The base node however will operate continuous.

LCD/Interface: Once sensor nodes have been “linked” and “joined” then information is available on the LCD screen at the base node. A simple one-button control is provided that allows the user to scroll through each node within range and displays temperature and pressure. Note that this is the information presently being transmitted, however any sensor could be used provided that it satisfies the following requirements: 1) Sends data via SPI output, 2) Connects to the provided SIP sockets on the sensor node PCB, and 3) Satisfies the height limitation inside the sensor node enclosure. One push of the button advances to the next node's information. One node is displayed at a time, and if a period of inactivity occurs, the LCD unit will go to sleep until the button is pushed to conserve power.

Power Supply: The power supply operates autonomously from the rest of the system. To power up, specific conditions must be met. First, the initial state of the batteries must be greater than 7V. Once operating it will continue to operate until the batteries drop below 6V. Note that the maximum input is 18V to the controller so any attempt to raise the bias of the supply will result in failure. All inputs to the supply are diode protected against accidental reverse hook-up. In addition, TVS protection is used to prevent damage to the microcontroller for ADC sampling of the battery and solar panel voltage.

5.0) Testing Procedures

5.1) Base Station Testing Procedures

5.1.1) Solar Panel Control System

The test procedures for the solar panel control system will involve the stepper motor setup, the mounting figuration, solar panel and MCU (PIC24). The solar panel will be checked for the maximum open circuit voltage output based on the result the step down resistive network may be altered. The code will be check for functionality and simulated in IPLAB. The solar panel reading will then be verified to check that the A/D function is working correctly. The next test will involve the integration of the code and stepper motor. The positioning of the stepper motor will be will tested with the placement a fixed protractor. The motor will have a thin polymer strip attached horizontally to the shaft of the motor so that when the motor is moved, its change in position can be measured. This test will then be performed with the full weight of the solar panel mount and calibrations will be performed if needed.

5.1.2) Maximum Power Point Tracking Test

Two flyback power supplies will be interfaced with separate solar panels. Each set-up will be identical, using the same solar panel, and positioned in the same relative location with a solar panel angle of 45 degrees; this will ensure minimized environmental variations. The control variable will be in regard to the MPP algorithm. In other words, one supply will utilize the tracking algorithm while the other will not. To reduce the significant source of error due to battery variations, the power supply units will be connected to fixed load resistors. The load resistors will be $13.4\ \Omega$ which simulates a power output of 75% of the maximum solar panel input power. A data acquisition unit will be used to sample the voltage (once per second), and indicate performance of both set-ups over a range of light conditions that vary throughout the day. The focus of this test will be to obtain a quantitative conclusion regarding the effectiveness of the MPP tracking algorithm.

5.1.3) Charger Performance Test

The battery charger performance is essential in order to judge the effectiveness of the base station power unit. A full day test will be conducted to observe charger performance over a typical day's environmental variations. The unit will be connected using the specified panel and battery combination. Solar Panel Voltage, Average Input Current, Battery voltage and Battery Charging current will be sampled once per second to observe the average values over time.

5.2) Sensor Node Hardware Testing Procedures

The sensor node has several components that are required for implementation. Each of the various parts must be built and tested separately before developing the overall PCB and placing components. The following outlines the testing procedures that are required for each section.

5.2.1) Solar Cell Harvesting Capability:

The sensor node must be capable of harvesting power from the solar cells. In order to verify that the solar cells are capable of harvesting adequate energy, a test circuit will be built on a breadboard and interfaced with a single cell. The solar cell and charging circuit were taken outdoors periodically to verify the functionality of the circuit; during sunlit hours, the supply voltage from the charging circuit was approximately 3.158 V, which is within the operating limits.

5.2.2) Battery Charging Circuit:

The battery that has been selected to supply the sensing nodes is a manganese lithium battery. It is capable of supplying 3.2 V with a life-span of 40mAh. To validate the charging recommendations provided by the supplier, a current limited voltage supply will be placed across the battery. Holding to these charging recommendations, the battery supply was adequately recharged from zero supply to the maximum supply in approximately 14 hours. Although this is well beyond our original goal of 4 hours of equivalent irradiation, during typical operation the battery will have on average less than 1.65 mA per hour. Since the solar cells can supply a recharge current of 22 mA,

it is assumed that with only four hours of irradiation, the panels will be adequately charged and never drop toward a zero state charge.

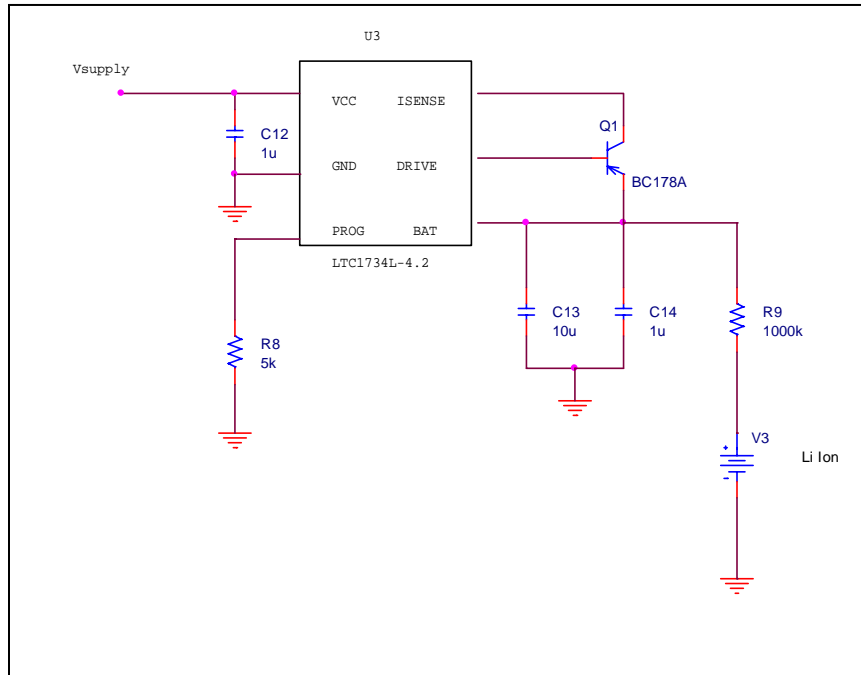


Figure 35: Alternative Sensor Charger With Lithium Ion Supply

5.2.3) Sensor Operation Verification

As described in section 3.4, the code to read the sensor node was verified by measuring the SPI and GPIO pins on the CC2430 and comparing these to the expected results according to the SCP 1000 datasheet. Also, comparing the temperature in various settings to the Fluke readout of a thermistor reading, it was determined that the sensor reading is accurate.

5.2.4) Communication:

After verifying that the sensors work properly, and the interface with the MCU is appropriate, the zigbee module will be placed in the circuit. Taking the sensor and base station communication circuits outdoors and onto the track, it was determined that the sensor node can communicate appropriately up to 100 yards.

The resulting flow for the sensor node testing procedure can be viewed in the figure below.

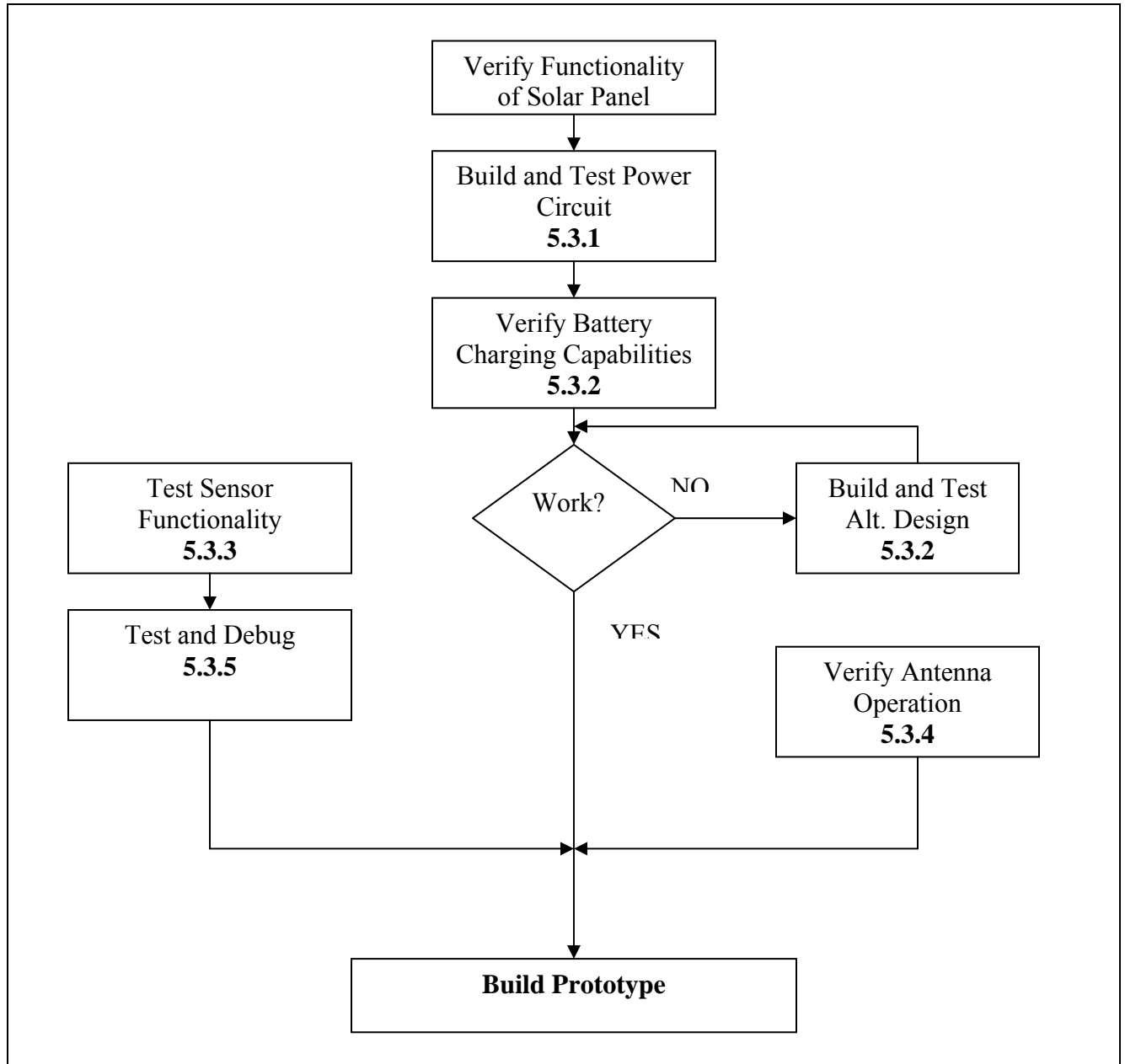


Figure 36: Testing Procedure Flow to Verify Sensor Node Operability

The software for each of the different nodes (i.e. base station and sensor modules) were testing by scoping the SPI and GPIO pins on the CC2430 to verify the functionality of the peripherals. Upon verifying these (see figure [37]), an LCD and push button was placed at the base station to verify that the code adequately cycles through each of the user's sensor data. Although we were unable to capture a photograph of the LCD before the display was ruined, the code was successfully demonstrated. By pressing a button, the user at the base station was able to cycle through and display information that was read at each of the remote sensor modules.

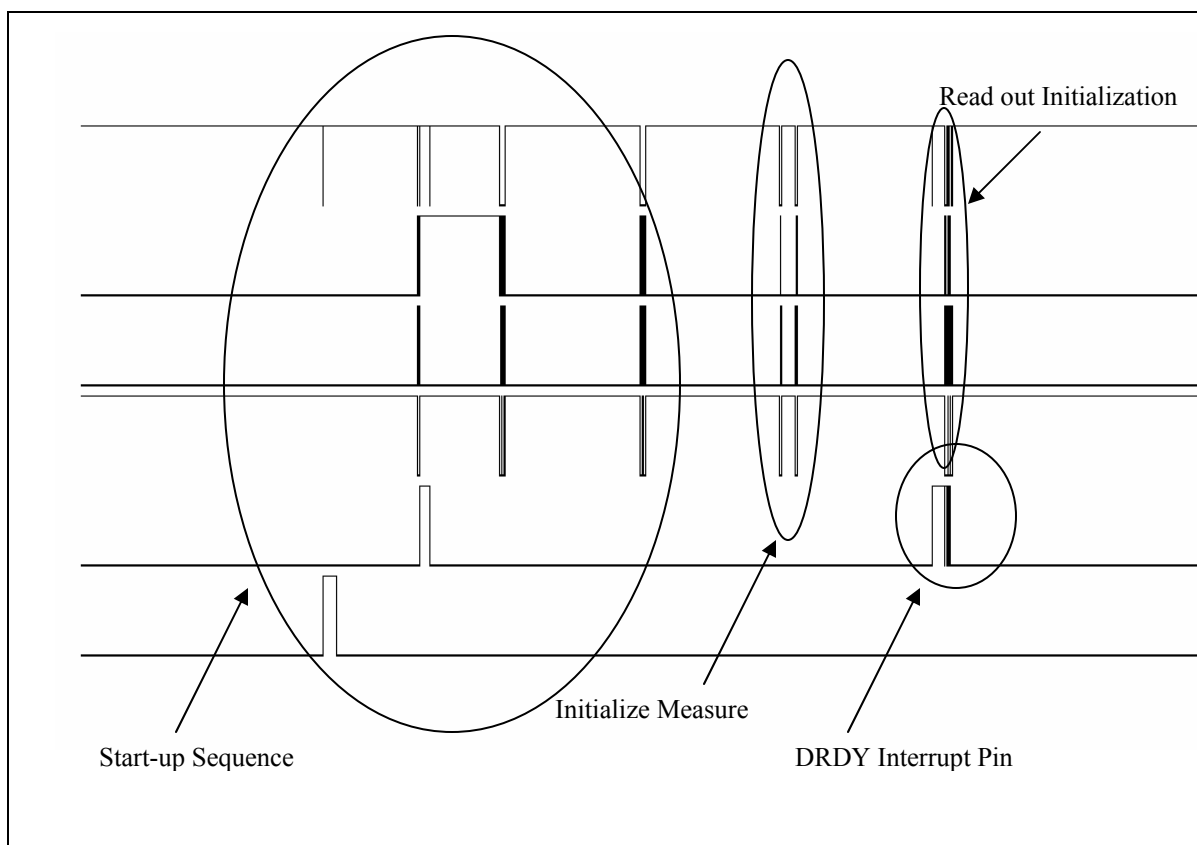


Figure 37: Sensor Node Peripheral and GPIO Readings

6.0) Financial Budget

The following tables outline two budgetary categories for this project. The first table covers the labor costs that are expected while the second encompasses the material cost.

6.1) Labor Costs

The labor cost table assumes that each person will work approximately 10 hours per week at a rate of \$10.00 per hour. The duration of the project is 15 weeks, thereby resulting in a total cost per person of \$1500.00.

Contributor	Total Hours (15 wk. semester)	Rate (\$/hr)	Ind. Cost
Josh Mahaffey	150	10	1500
Jeff Petermann	150	10	1500
Ben McDonald	150	10	1500
Jacob Pozderac	150	10	1500
Total Cost			6000

Table 6: Labor Costs

6.2) Material Cost





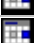



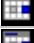



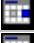



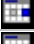


The materials required for the project are outlined in the table below. The materials encompass every aspect of the design: electrical and mechanical considerations at the base station, data node, and sensor node.

Final Project Budget Breakdown					
Part	Description	Cost	Quantity	Total	
CC2430EMK	TI's communications evaluation module	\$50.00	3	\$150.00	Donated
SCP1000	VTI's combined pressure/temperature sensor	\$57.08	2	\$114.16	
LDO	Microchip adjustable drop-out regulator	\$0.42	3	\$1.26	
SP4.2-37	PowerFilm 4.2 V, 22 mA solar panel	\$5.00	2	\$10.00	
ML2020	Magenese Lithium battery rated for 3.0 V at 40 mAh	\$2.68	4	\$10.72	
78MOS	Stepper Motor	\$300.00	1	\$300.00	Donated
PCB	3 Printed Circuit Boards	\$60.00	1	\$60.00	
R208	Stepper Motor Driver Module	\$89.00	1	\$89.00	
DEMULINE	Arduino Chip	\$30.00	1	\$30.00	
612FL	Power Supply Fan	\$19.60	1	\$19.60	
MAX232	Signal Boost for Serial Communication	\$0.89	1	\$0.89	
27979	Parallax Inc. LCD	\$34.25	1	\$34.25	
DSP-1012	Solar Panel	\$119.00	2	\$238.00	
	Power Source	\$35.51	1	\$35.51	
	Plexiglass	\$2.67	2	\$5.34	
	12V 5.1Ah Sealed Lead Acid Battery	\$25.00	3	\$75.00	Donated
	Terminal Block	\$5.00	1	\$5.00	
	L-Brackets	\$0.96	9	\$8.64	
	Angled Aluminum	\$53.00	1	\$53.00	
	Fiberglass and Materials	\$325.59	1	\$325.59	
	2ft. SMA Extension Cable	\$29.00	1	\$29.00	
	Power Source Shielding	\$8.48	1	\$8.48	
	Brush Holder	\$8.28	2	\$16.56	
	System Fastening Hardware	\$50.00	1	\$50.00	
	Push Button	\$6.49	1	\$6.49	
	Rocker Switch	\$1.49	1	\$1.49	
	System Connectors	\$25.00	1	\$25.00	
		Total		\$1,702.98	

Table 7: Parts and Material Costs

7.0) Project Schedules

The project schedule has been divided into two categories. The first, shown in table _ (the design gantt chart), outlines the scheduling of the design phase. The table shown in figure 31 (implementation gantt) shows the dates and deadlines of the implementation and prototyping phase of the project.

ID		Task Name	Duration	Start	Finish	Predec
63		Construct Solar Panel Mount/Motor	1 day	Fri 8/29/08	Sat 8/30/08	
64		Buck/Boost Power Supply	49 days	Fri 10/17/08	Fri 12/5/08	
65		Derive MPP Algorithm for DCM Mo	7 days	Fri 10/17/08	Fri 10/24/08	
66		Inductor Calculations	7 days	Fri 10/24/08	Fri 10/31/08	
67		Circuit Design	7 days	Fri 10/31/08	Fri 11/7/08	
68		Prototype Design	7 days	Fri 11/7/08	Fri 11/14/08	
69		Verify Prototype Design	7 days	Fri 11/14/08	Fri 11/21/08	
70		Field Test: Data Logger?	7 days	Fri 11/21/08	Fri 11/28/08	
71		Evaluate Test Data / Final Design	7 days	Fri 11/28/08	Fri 12/5/08	
72		Zigbee Transmission	7.63 days	Tue 10/14/08	Wed 10/22/08	
73		Zigbee Module	4 days	Tue 10/14/08	Sat 10/18/08	
74		Zigbee Antenna	4 days	Sat 10/18/08	Wed 10/22/08	
75		Astronaut Interface	7 days	Mon 10/20/08	Mon 10/27/08	
76		LCD Display	4 days	Mon 10/20/08	Fri 10/24/08	
77		User Control	3 days	Fri 10/24/08	Mon 10/27/08	76
78		Mechanics	1 day	Fri 8/29/08	Sat 8/30/08	
79		Structural Plan	1 day	Fri 8/29/08	Sat 8/30/08	
80		Layout	1 day	Fri 8/29/08	Sat 8/30/08	
81		Antenna/Power Calculations	1 day	Fri 8/29/08	Tue 9/2/08	
82						
83		Data Node	49 days	Fri 10/17/08	Fri 12/5/08	
84		Power Requirements at Receiver	10 days	Fri 10/24/08	Mon 11/3/08	
85		Solar Panel	14 days	Fri 11/21/08	Fri 12/5/08	
86		Electrical Characteristics	14 days	Fri 11/21/08	Fri 12/5/08	
87		Physical Characteristics (size, weight, et	14 days	Fri 11/21/08	Fri 12/5/08	
88		Battery	14 days	Fri 11/21/08	Fri 12/5/08	
89		Antenna/Power Calculations	7 days	Mon 11/3/08	Mon 11/10/08	84
90		Zigbee Transmission	35 days	Fri 10/17/08	Fri 11/21/08	
91		Zigbee Module	21 days	Fri 10/17/08	Fri 11/7/08	
92		Zigbee Antenna	10 days	Mon 11/3/08	Thu 11/13/08	84
93		Transmitting Circuit and Schematic	21 days	Fri 10/31/08	Fri 11/21/08	
94		Receiver Circuit and Schematic	21 days	Fri 10/24/08	Fri 11/14/08	
95						
96		Sensor Node (Temperature, Pressure, a	61 days	Fri 10/3/08	Wed 12/3/08	
97		Power Requirements at Sensor Node	31 days	Fri 10/3/08	Mon 11/3/08	
98		Sensor Power Supply	24 days	Fri 10/31/08	Mon 11/24/08	




















ID		Task Name	Duration	Start	Finish	Predec
99		Investigation of Power Sources (Solar and Piezoelectric)	14 days	Fri 10/31/08	Fri 11/14/08	
100		Feasability Study of Power Sources	14 days	Fri 10/31/08	Fri 11/14/08	
101		Complete a study of size vs. hardware	3 days	Fri 10/31/08	Mon 11/3/08	
102		Complete a study of size and requirements	7 days	Fri 10/31/08	Fri 11/7/08	
103		Develop a cost analysis spreadsheet	7 days	Fri 11/7/08	Fri 11/14/08	102
104		Finalize a cost and distributor list	0 days	Fri 11/14/08	Fri 11/14/08	103
105		Circuit Schematics for Supply Power	24 days	Fri 10/31/08	Mon 11/24/08	
106		Circuit Analysis of Current Harvesting	14 days	Fri 10/31/08	Fri 11/14/08	
107		Solar Cell Supplies	10 days	Fri 10/31/08	Mon 11/10/08	
108		Piezoelectric Supplies	7 days	Fri 11/7/08	Fri 11/14/08	
109		Develop Sensor Supply Schematics	14 days	Mon 11/10/08	Mon 11/24/08	
110		Utilize understanding of above	14 days	Mon 11/10/08	Mon 11/24/08	
111		Solar Cell Supply (For Temperature)	10 days	Mon 11/10/08	Thu 11/20/08	
112		Piezoelectric Supply (For Temperature)	10 days	Fri 11/14/08	Mon 11/24/08	
113		Transmission Antenna	7 days	Fri 11/21/08	Fri 11/28/08	
114		Determine the necessary antenna characteristics	7 days	Fri 11/21/08	Fri 11/28/08	
115		Determine the impedance seen by the load	1 day	Fri 11/21/08	Sat 11/22/08	
116		Develop (if necessary) matching circuit and antenna	7 days	Fri 11/21/08	Fri 11/28/08	
117		Finalize a cost and supplier for the requirements	0 days	Fri 11/28/08	Fri 11/28/08	116
118		Zigbee Transmission	12 days	Fri 11/21/08	Wed 12/3/08	
119		Zigbee Module	1 day	Fri 11/21/08	Sat 11/22/08	
120		Incorporate associated circuitry in schematics	5 days	Fri 11/28/08	Wed 12/3/08	
121						
122						
123						
124		Parts Request Form	486.04 days?	Fri 8/29/08	Mon 12/28/09	
130		Design Gantt Chart	14 days	Mon 10/20/08	Mon 11/3/08	35
131		Project Poster	7 days	Mon 11/3/08	Mon 11/10/08	130
132		Implementation Gantt Chart	21 days	Mon 11/10/08	Mon 12/1/08	131
133		Final Design Report	89 days	Fri 8/29/08	Wed 11/26/08	
134		Final Design Presentation	9 days	Wed 11/26/08	Fri 12/5/08	133

Figure 38: Project Design Schedule

ID		Task Name	Duration	Start	Finish	Predecessors
1		Software Design	35 days	Mon 2/2/09	Fri 3/20/09	
2		Program Zigbee Chips	15 days	Mon 2/2/09	Fri 2/20/09	
3		Develop SPI Interface to Zigbee Chips	15 days	Mon 2/2/09	Fri 2/20/09	
4		Create Macros for settings for each chip	15 days	Mon 2/2/09	Fri 2/20/09	
5		Software Development	20 days	Mon 2/23/09	Fri 3/20/09	
6		Base Node	10 days	Mon 2/23/09	Fri 3/6/09	
7		SPI Interface with Zigbee Chip	10 days	Mon 2/23/09	Fri 3/6/09	
8		UART Interface with LCD Display	10 days	Mon 2/23/09	Fri 3/6/09	
9		Data Node	10 days	Mon 2/23/09	Fri 3/6/09	
10		Sensor Node	10 days	Mon 3/9/09	Fri 3/20/09	
11		SPI Interface with Zigbee Chip	10 days	Mon 3/9/09	Fri 3/20/09	
12		SPI Interface with Sensor	10 days	Mon 3/9/09	Fri 3/20/09	
13						
14		Hardware Design	86 days	Mon 12/15/08	Mon 4/13/09	
15		Base Node	62 days	Mon 1/12/09	Tue 4/7/09	
16		Power Supply / Voltage Regulator	62 days	Mon 1/12/09	Tue 4/7/09	
17		Verify Prototype Operation: (Supply Circuit)	6 days	Mon 1/12/09	Mon 1/19/09	
18		Verify Prototype Operation: (Algorithm1)	6 days	Mon 1/19/09	Mon 1/26/09	
19		Verify Prototype Operation: (Algorithm2)	6 days	Mon 1/26/09	Mon 2/2/09	
20		Field Test for MPP	6 days	Mon 2/9/09	Mon 2/16/09	
21		Analyze Data from Field Test	6 days	Mon 2/16/09	Mon 2/23/09	
22		Possible Corrections: Tweak Algorithm	6 days	Mon 2/23/09	Mon 3/2/09	
23		Re-Test / Verify	6 days	Mon 3/2/09	Mon 3/9/09	
24		Analyze Data: Test 2	6 days	Mon 3/9/09	Mon 3/16/09	
25		Final Assembly: Interconnects/Housing	6 days	Mon 3/16/09	Mon 3/23/09	
26		Finalize Report	6 days	Mon 3/23/09	Mon 3/30/09	
27		Emergency Back-up Tasks	7 days	Mon 3/30/09	Tue 4/7/09	
28		Communication Circuit	40 days	Mon 1/12/09	Fri 3/6/09	
29		Test Antenna on VNA	7 days	Mon 1/12/09	Tue 1/20/09	
30		Determine Matching Components	1 day	Wed 1/21/09	Wed 1/21/09	29
31		Build Communication Circuit (With Matching	7 days	Thu 1/22/09	Fri 1/30/09	30
32		Interface With MCU	1 day	Mon 2/2/09	Mon 2/2/09	31
33		Test Transmission Distance	5 days	Tue 2/3/09	Mon 2/9/09	32
34		Debug	14 days	Tue 2/10/09	Fri 2/27/09	33
35		Finalize	0 days	Fri 2/27/09	Fri 2/27/09	34
36		Solar Panel Control System	40 days	Mon 1/12/09	Fri 3/6/09	
37		Solar Panel Mount Construction	15 days	Mon 1/12/09	Fri 1/30/09	
38		Programming Stepper Motor Control Sys	15 days	Mon 1/12/09	Fri 1/30/09	
39		Angle Positioning Calibration	10 days	Mon 1/26/09	Fri 2/6/09	
40		Solar Panel Control System Testing (wit	15 days	Mon 1/26/09	Fri 2/13/09	
41		Debug	15 days	Mon 2/16/09	Fri 3/6/09	40
42		Finalize	15 days	Mon 2/16/09	Fri 3/6/09	
43						

ID		Task Name	Duration	Start	Finish	Predecessors
41		Debug	15 days	Mon 2/16/09	Fri 3/6/09	40
42		Finalize	15 days	Mon 2/16/09	Fri 3/6/09	
43						
44						
45		Data Node	66 days	Mon 1/12/09	Mon 4/13/09	
46		Communication Circuit	35 days	Mon 1/12/09	Fri 2/27/09	
47		Test Antenna on VNA	7 days	Mon 1/12/09	Tue 1/20/09	
48		Determine Matching Components	1 day	Wed 1/21/09	Wed 1/21/09	47
49		Build Communication Circuit (With Matching	7 days	Thu 1/22/09	Fri 1/30/09	48
50		Interface With MCU	1 day	Mon 2/2/09	Mon 2/2/09	49
51		Test Transmission Distance	5 days	Tue 2/3/09	Mon 2/9/09	50
52		Debug	14 days	Tue 2/10/09	Fri 2/27/09	51
53		Finalize	0 days	Fri 2/27/09	Fri 2/27/09	52
54		Solar Power Development	14 days	Mon 1/12/09	Thu 1/29/09	
55		Build Solar Power Regulator Circuit	2 days	Mon 1/12/09	Tue 1/13/09	
56		Debug	5 days	Wed 1/14/09	Tue 1/20/09	55
57		Interface With Solar Cell	2 days	Wed 1/21/09	Thu 1/22/09	56
58		Field Test	5 days	Fri 1/23/09	Thu 1/29/09	57
59		Finalize	0 days	Thu 1/29/09	Thu 1/29/09	58
60		Interface Solar Power Supply and Comm. Circu	14 days	Mon 3/2/09	Thu 3/19/09	
61		Test and Debug	14 days	Mon 3/2/09	Thu 3/19/09	53
62		Develop PCB Layout	5 days	Fri 3/20/09	Thu 3/26/09	61
63		Solder Components	5 days	Fri 3/27/09	Thu 4/2/09	62
64		Test and Debug	7 days	Fri 4/3/09	Mon 4/13/09	63
65						
66		Sensor Node	77 days	Mon 12/15/08	Tue 3/31/09	
67		Antenna Design	21 days	Mon 12/15/08	Mon 1/12/09	
68		Develop Printed Circuit Antenna Parameters	7 days	Mon 12/15/08	Tue 12/23/08	
69		Simulate With Radiation Simulator (HFSS, AI	7 days	Wed 12/24/08	Thu 1/1/09	68
70		Design Test Antenna	0 days	Thu 1/1/09	Thu 1/1/09	69
71		Perform S-Parameter Evaluation	7 days	Fri 1/2/09	Mon 1/12/09	70
72		Finalize	0 days	Mon 1/12/09	Mon 1/12/09	71
73		Solar Power Development	15 days	Tue 1/13/09	Mon 2/2/09	
74		Create Regulator Circuitry	4 days	Tue 1/13/09	Fri 1/16/09	72
75		Test Regulator (Breadboard Circuit)	1 day	Mon 1/19/09	Mon 1/19/09	74
76		Debug	5 days	Tue 1/20/09	Mon 1/26/09	75
77		Field Test With Solar Panel	5 days	Tue 1/27/09	Mon 2/2/09	76
78		Finalize	0 days	Mon 2/2/09	Mon 2/2/09	77
79		Battery Charger	27 days	Mon 2/9/09	Tue 3/17/09	
80		Regulator Charging Tests (Monitor Charging)	7 days	Mon 2/9/09	Tue 2/17/09	
81		Determine Effectiveness	3 days	Wed 2/18/09	Fri 2/20/09	80
82		Alternate Design (If Necessary)	17 days	Mon 2/23/09	Tue 3/17/09	
86		Finalize	0 days	Tue 3/17/09	Tue 3/17/09	81,85



ID		Task Name	Duration	Start	Finish	Predecessors
87		Sensor Evaluation	24 days	Tue 1/13/09	Fri 2/13/09	
88		Build Sensor, MCU Circuit	5 days	Tue 1/13/09	Mon 1/19/09	72
89		Program Sensor MCU	14 days	Tue 1/20/09	Fri 2/6/09	88
90		Evaluate Accuracy	5 days	Mon 2/9/09	Fri 2/13/09	89
91		Communication Circuit	8 days	Mon 2/16/09	Wed 2/25/09	
92		Interface Zigbee Chip With Sensors	1 day	Mon 2/16/09	Mon 2/16/09	90
93		Testing Comm. Distances (Whip Antenna)	7 days	Tue 2/17/09	Wed 2/25/09	92
94		Create PCB Layout	7 days	Mon 2/16/09	Tue 2/24/09	90
95		Solder Components	7 days	Tue 3/3/09	Wed 3/11/09	
96		Test and Debug	14 days	Thu 3/12/09	Tue 3/31/09	95

Table 39: Implementation and Prototyping Schedule

8. Design Team Information

Team Manager: Joshua Mahaffey
e-mail: jvm5@uakron.edu
Major: Electrical Engineering
Design Responsibility: Sensor Nodes and Antenna Designs

Archivist: Jeff Petermann
e-mail: jcp16@uakron.edu
Major: Electrical Engineering
Design Responsibility: Max Power Point Tracking Algorithm and Base Station Power Supply.

Software Manager: Jacob Pozderac
e-mail: jpozz321@gmail.com
Major: Computer Engineering
Design Responsibility: Main (and other) MCU Programming and Zigbee Communications Protocol Lead

Hardware Manager: Ben McDonald
e-mail: bam28@uakron.edu
Major: Electrical Engineering
Design Responsibility: Mechanical Design and Motor Control for Base Station Solar Panel

9.0) Conclusions and Recommendations

NASA has a requirement and direct application for a wireless sensing network that is capable of harvesting power from the surrounding environment. Although the application that the system has been designed for is for sensing on extraterrestrial surfaces, the design that has been implemented has little regard given to temperature constraints and other environmental constraints. Our goal has been to merely prove the concept of a wireless sensing system. As a result, the application of such a system is broad and could be utilized for a variety of situations in aerospace, military, consumer electronics, industry, and a plethora of other areas. The principles and theories presented are applicable to all conceivable applications; however, the sensors and materials utilized must be carefully considered and will vary depending upon the function.

Many types of harvesting techniques have been considered for the implementation of this project; however, due to time constraints as well as monetary concerns, the harvesting technique that has been selected is via solar cells. It is important to realize that other techniques are just as valid as photo voltaics and could encompass the following categories:

- Piezoelectrics (vibration harvesting)
- Ambient and Direct RF Harvesting (SAW Devices)
- Pyroelectrics (temperature harvesting)
- Hydro Power (harvesting the energy of moving water)

Now that the concept has been proven utilizing solar energy, the goal of future work would be to create application specific designs wherein the environment is an integral part of the proposed constraints. Also, further research and design could be carried out in order to implement other types of harvesting techniques.

Appendix A: Matlab Scripts and Plots for Determining Power Supply Constraints

Solar Panel Parameters	a
Variables	a
Relationships.....	a
Power Supply Input Impedance:.....	b
Plotting = Panel.....	b
Plotting = Converter Impedance	c

Solar Panel Parameters

The following parameters are for a BPSolar 20W panel directly from its datasheet and using Ortiz. Subsequent calcs fully define its Vop and current for a given set of conditions. This simulation has been carried out at standard external conditions for its full range of output voltages.

```
Pmax = 20;
Vmop = 16.8; %V @ Pmax
Imop = 1.19; %I @ Pmax
Voc = 21; %Open Circuit Voltage
Vmax = Voc*1.03; %At 1200W/m^2, or est 1.03xVoc
Vmin = Voc*.85; %At 200W/m^2, or est .85xVoc
Isc = 1.29; %Short Circuit Current
Ein = 1000; %Standard Conditions, W/m^2
Tn = 25; %Degrees C, Stand Conditions
TCV = -.08; %percent volts per degree C
TCI = .065; %percent current per degree C
b = .05; %PVM characteristic? P temp coeff
%*****
% Parameter b was derived, but sometimes it is provided by manufacturers.
%*****
```

Variables

Standard Operating Conditions For Light & Temperature

```
Ei = 1000; %Irradiation (W/m^2)
T = 25; %Ambient Temperature
V = [.01: 1: Voc]; %Tested Range of Voltage
```

Relationships

First the min and max values need to be determined for open and short circuit conditions. The characteristics of the solar panel define the points between these two operating corners.

```
% Equation[S1]: Voltage for Standard Operating Conditions
Vx = (Ein./Ei)*TCV*(T-Tn)+Vmax-(Vmax-Vmin)*exp((Ein./Ein)*log((Vmax-Voc)/(Vmax-
Vmin)));

% Equation[S2]: Current for Standard Operating Conditions
Ix = (Ein./Ein)*(Isc+(TCI*(T-Tn)));

% Notes:
% 1) Vx is the open circuit voltage for a given T and Ei.
% 2) Ix is I short circuit for given T or Ei.
%*****
%(Relations as functions of voltage - I(v), P(v), Rop)
%Equation[S3]: Current as a function of Voltage
Iv = (Ix/(1-exp(-1/b))).*(1-exp((V./(b*Vx))-(1/b)));

%Equation[S4]: Power as function of Voltage
```

```

Pv = V.*Iv;
%Equation[S5]: Operating Point(Impedance) of PVM
Rop = V./Iv;

%Reference:
%Ortiz-Rivera, Eduardo, "Maximum Power Point Tracking Using the Optimal Duty Ratio
for DC-DC
%Converters and Load Matching in Photovoltaic Applications", Applied Power
%Electronics Conference and Exposition, 2008

```

Power Supply Input Impedance:

Input Impedance by Equation: $R_i = (2 \cdot L \cdot T_s) / T_{on}^2$

```

L           = 80e-6;
%Tsmx       = 37.5e-6;
%Tsmn       = 16.67e-6;
Ts          = [16.5e-6:1e-6:37.5e-6];
Ton1        = .5.*Ts; %50% Duty Cycle (Chosen to demonstrate).
Ton2        = .75.*Ts; %75% Duty
Ton3        = .95.*Ts; %Max Duty Cycle system allows

Ri1         = (2*L).*(Ts./Ton1.^2);
Ri2         = (2*L).*(Ts./Ton2.^2);
Ri3         = (2*L).*(Ts./Ton3.^2);

```

Plotting = Panel

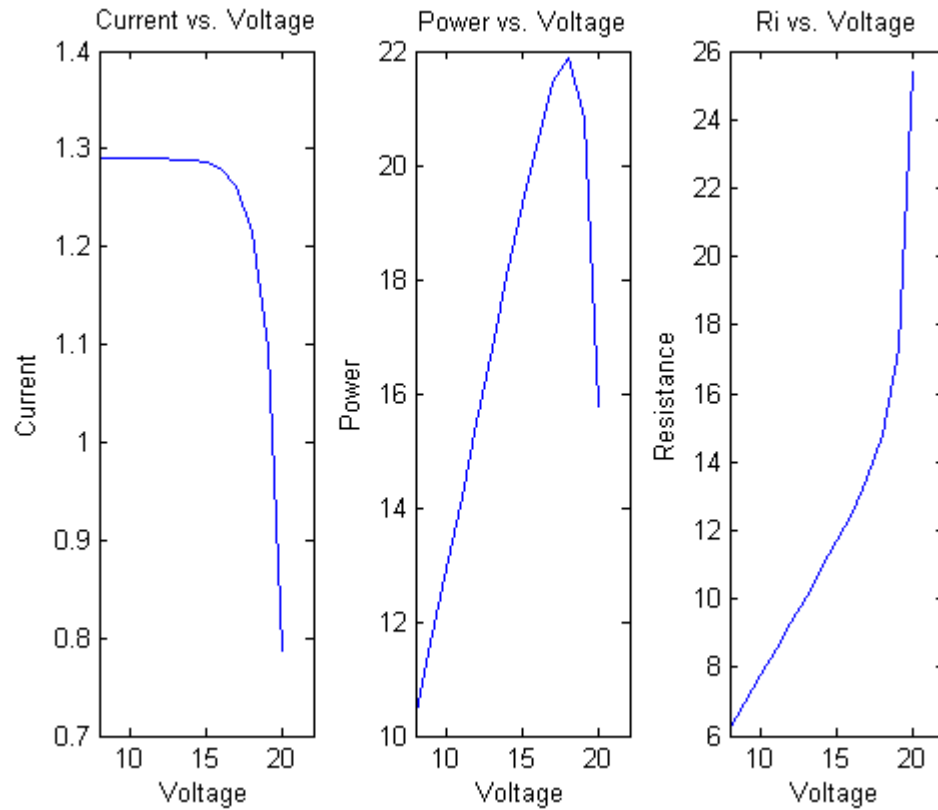
```

figure(1)
%sol arplot(V,Iv,Pv,Rop)
subplot(1,3,1)
plot(V,Iv); xlabel('Voltage'); ylabel('Current');
title('Current vs. Voltage'); xlim([8 22]);

subplot(1,3,2)
plot(V,Pv); xlabel('Voltage'); ylabel('Power');
title('Power vs. Voltage'); xlim([8 22]);

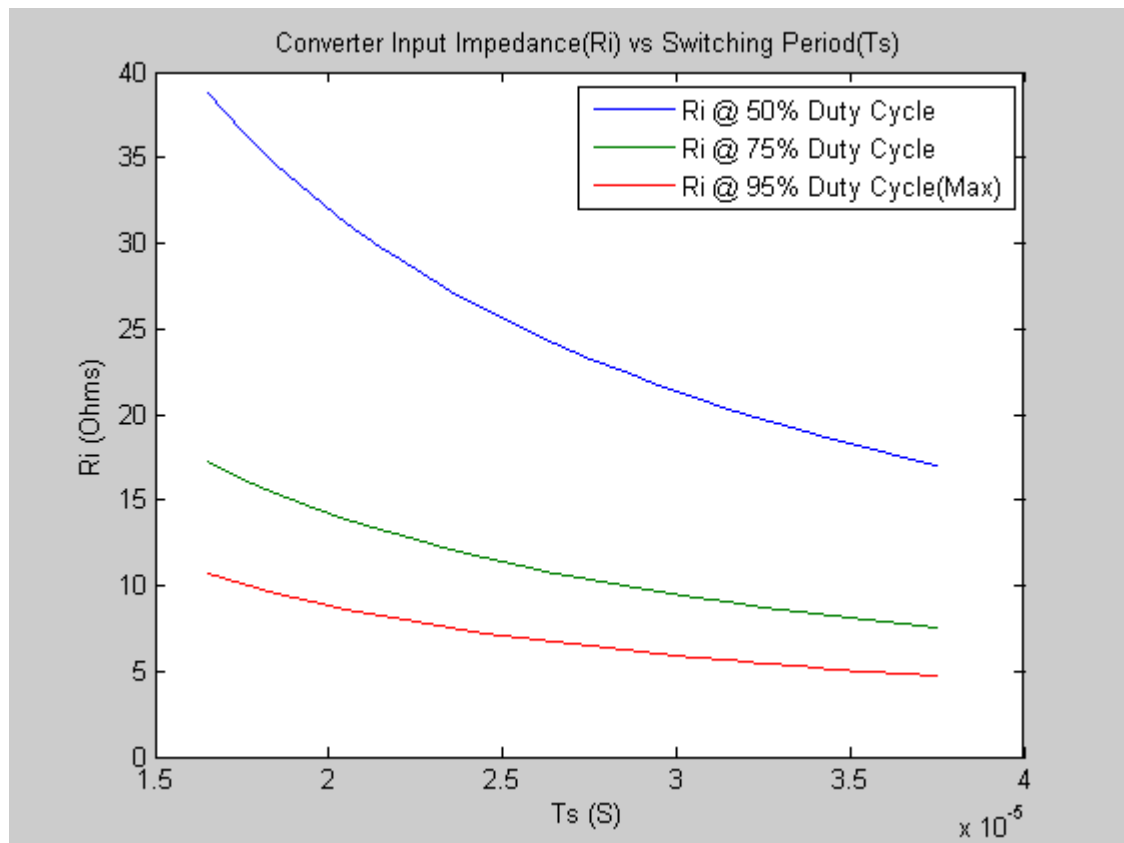
subplot(1,3,3)
plot(V,Rop); xlabel('Voltage'); ylabel('Resistance');
title('Ri vs. Voltage'); xlim([8 22]);

```

Plotting = Converter Impedance

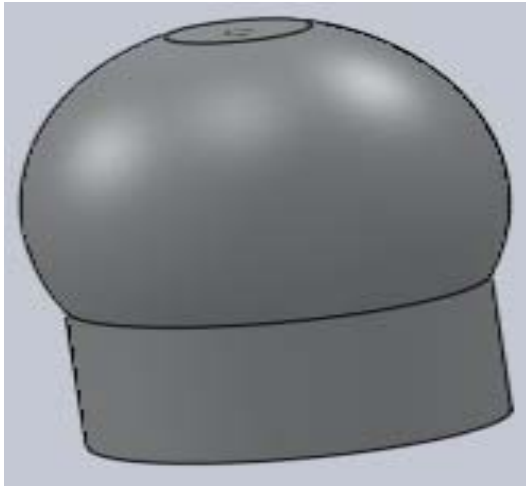
```
figure(2)
plot(Ts, RI 1, Ts, RI 2, Ts, RI 3)
xlabel('Ts (S)'); ylabel('RI (Ohms)')
legend('RI @ 50% Duty Cycle', 'RI @ 75% Duty Cycle', ...
       'RI @ 95% Duty Cycle(Max)');
title('Converter Input Impedance(RI) vs Switching Period(Ts)');
```



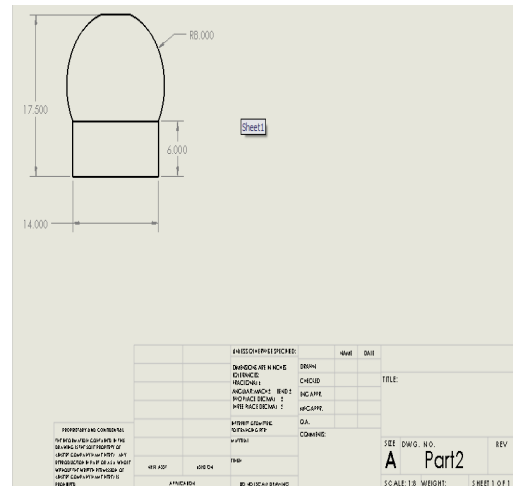
Appendix B: Mechanical Assemblies and Enclosure Details

The enclosure was made of fiber glass and was designed in a way that would allow the stepper motor to be fully supported. A dome-like structure was decided to give the largest support for a stepper motor mounted at the top. The solar panels were hinged to an aluminum frame and supported by the stepper motor rod. The following figures depict much of the mechanical assembly work.

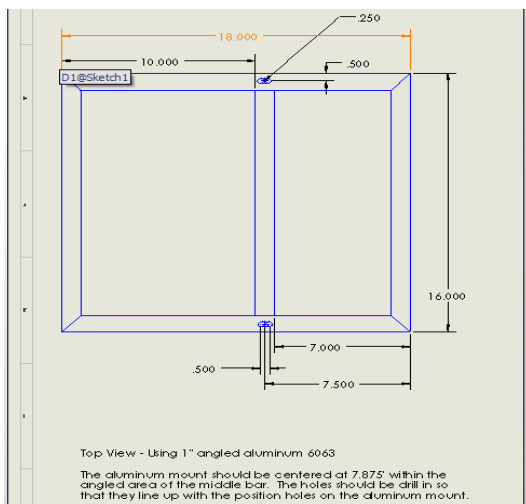
The last mechanical innovation that would allow the solar panels to rotate without the solar panel wire affecting any of the outer pieces was the use of two ringed conductors placed outside and at the top of the enclosure. These conductors were wired directly to the internal circuitry and dc motor brushes were connected to the solar panel wiring and aluminum frame. As the panels are rotated, the brushes slide along the conductors and allow the panel voltage to be read.



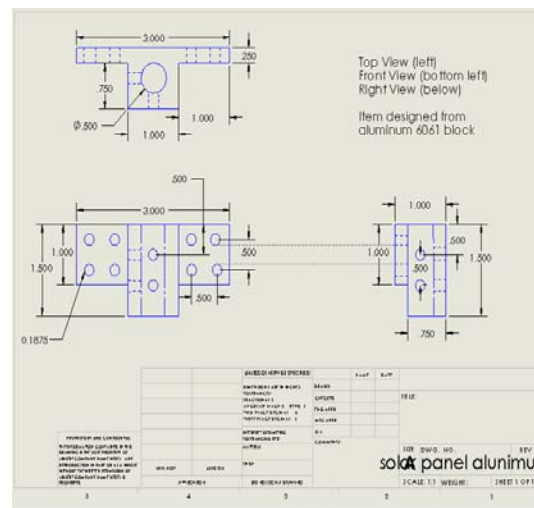
Enclosure Composition 3-D Diagram



Enclosure Composition Dimension



Solar Panel Rack Mount Dimension



Stepper Motor Mechanical Coupling Device Dimension